

Exploring a New Design Paradigm for Omnidirectional MAVs for Minimal Actuation and Internal Force Elimination: Theoretical Framework and Control

Ahmed Ali*, Quentin Sablé*, Chiara Gabellieri*, Antonio Franchi*^{*,†}

Abstract—This paper presents a novel concept for achieving omnidirectionality in a multirotor aerial vehicle (MAV) that uses only 6 inputs and ensures no internal forces at the equilibria. The concept integrates a single actively-tilting propeller along with 3 pendulum-like links, each carrying a propeller, connected by passive universal joints to the main body. We show that this design ensures omnidirectionality while minimizing the internal forces and without resorting to overactuation (i.e., more than 6 inputs). A detailed dynamic model of the multi-link MAV is first developed. Afterwards, the analysis identifies the equilibrium configurations and illustrates that a forced equilibrium exists for every pose of the MAV’s main platform. In order to render this equilibrium asymptotically stable for the closed-loop system, a coordinate-invariant nonlinear controller is constructed using dynamic feedback linearization and backstepping techniques with the main platform configuration error being the left-trivialized error on $SE(3)$. The stability of the closed-loop system is then investigated by employing standard Lyapunov arguments on the zero dynamics. We conclude by providing numerical Gazebo simulations, whose videos are available at <https://youtu.be/SWIt0CSwNUo>, validating our approach. They demonstrate the MAV capability to perform decoupled attitude and translational motions under parametric uncertainty and actuators noise.

NOMENCLATURE

$SE(3)$ Special Euclidean group of rigid-body transformations.
 $se(3)$ Lie algebra of $SE(3)$.
 \mathbb{T}^n n -torus manifold (a compact Lie group).
 $C_j^0 \in SE(3)$ Configuration of B_j ’s frame \mathcal{F}_{p_j} in the world frame \mathcal{F}_w .
 $V_1^0 \in \mathbb{R}^6$ Right-invariant base twist expressed in, and relative to, \mathcal{F}_w .
 $[\ast] : \mathbb{R}^6 \rightarrow se(3)$ An isomorphism with an inverse $\hat{\ast}$.
 $(\ast)_\times$ A skew-symmetric matrix of vector $\ast \in \mathbb{R}^3$.
 J_{1j} Universal joint connecting the base to link B_j .
 $S_j \in \mathbb{R}^{6 \times 2}$ J_{1j} ’s spatial instantaneous screw axis, $S_j = (S_{j1} \ S_{j2})$.
 $S_p = \text{blkdiag}(S_j)$ Block-diagonal matrix of screws S_j .
 $\text{Ad}_C : SE(3) \times se(3) \rightarrow se(3)$ Adjoint representation of $SE(3)$.
 $\text{ad}_V : se(3) \times se(3) \rightarrow se(3)$ Adjoint representation of $se(3)$.
 $R_k(\ast)$ Pure rotation about axis k by an angle \ast .
 e_i zero vector with one in index i .
 M Generalized mass (inertia) matrix.
 M_{bb}, M_{bp}, M_{pp} Base, coupling, and joint sub-matrices of M .

* Robotics and Mechatronics Department, Electrical Engineering, Mathematics, and Computer Science (EEMCS) Faculty, University of Twente, 7500 AE Enschede, The Netherlands. ahmed.ali@utwente.nl, q.l.g.sable@utwente.nl, c.gabellieri@utwente.nl, schol@r-franchi.eu

[†]Department of Computer, Control and Management Engineering, Sapienza University of Rome, 00185 Rome, Italy. schol@r-franchi.eu

This work was partially funded by the Horizon Europe research agreement no. 101120732 (AUTOASSESS).

h Centrifugal and Coriolis terms.

g_b, g_p Gravitational terms of base and joints, $g = (g_b \ g_p)^T$.

$W_{\text{app},b}^0$ Applied wrench on base’s CoM expressed in \mathcal{F}_w .

$W_{\text{app},p}^0$ Applied wrench on links B_2, B_3, B_4 ’s CoM expressed in \mathcal{F}_w and projected onto the respective joints through the corresponding screw in S_p .

τ_{dr_i} Drag torque about propeller i ’s axis.

$\tau_{f_{j_i}}$ Viscous friction at joint q_{j_i} ’s axis. $\bar{\tau}_f = (0_{6 \times 1} \ \text{col}(\tau_{f_{j_i}}))^T$

τ_{s_j} Torsion spring torque applied at joint q_{j_1} ’s axis.

τ_{d_j} Propeller j ’s drag torque factorized on q_{j_1} ’s axis at equilibrium.

m_b, m_j Mass of base and link B_j .

c Length from joints axes intersection point to B_j ’s CoM.

k_i Drag-to-thrust ratio of propeller i .

PJD₁, PJD₂ Passive-joint designs type 1 and type 2.

$P_{se(3)}(A)$ projects a matrix $A \in \mathbb{R}^{4 \times 4}$ on $se(3)$.

\ast_e Variable \ast evaluated at equilibrium.

$\ast^{[i]}$ Value of variable \ast pertaining to joint design PJD _{i} .

I. INTRODUCTION

Nowadays, Multirotor Aerial Vehicles (MAVs) are widely used in a variety of applications, ranging from agriculture to civil engineering [1]. Interest in this technology is growing, geared by its potential to perform tasks that require physical interaction with environments inaccessible to other types of mobile vehicles [2], [3]. While conventional quadrotors can efficiently handle some of these tasks, particularly when special orientation maneuvers are not required, certain applications have emerged in which the capability of executing decoupled translational and rotational motions is essential, necessitating the demand for new MAV designs since quadrotor dynamics inherently prohibits this kind of motion. One notable example where the MAV platform needs to maintain constant orientation while translating in space is the contact-based inspection of sloped surfaces [4], [5].

A. Research Problems and Related Work

When designing a new MAV, one can easily be convinced that it is desirable to obtain all the angular velocities of the propellers aligned with each other and with the gravity force at any static hovering equilibrium: this avoids internal propeller-generated forces canceling each other at the cost of a higher energy consumption; moreover, it is desirable to keep the number of actuators to the minimum (equal to the task dimension), to reduce the payload (which, in turn, affects

the vehicle’s endurance), the cost, the maintenance requirements, etc. Furthermore, for tasks requiring high dexterity like the ones mentioned before, it is desirable for the MAV to be able to statically hover at any pose (in $SE(3)$ in general). Last but not least, the design of a MAV must also allow the controlled stabilization of its hovering equilibria. We label these four desirable properties as the Internal-force Property, the Input-dimension Property, the Equilibria Property, and the Stabilizability Property, respectively.

When restricting the problem to the vertical 2D space, we demonstrated in [6] that a MAV design with all the above four properties exists. Especially, it can be stabilized at any static equilibrium pose in $SE(2)$ with propellers parallel to each other and the gravity vector, and it has only three actuators. The actuators are two brushless motors attached to one propeller each and one servomotor that actively tilts one of the two propellers, while the other one is free to passively rotate and has a center of mass not coincident with the rotation point. However, extending such a result to the 3D space is very far from being trivial and is an open problem. Just to mention two obstacles to such extension: $SE(3)$ is a fundamentally different manifold than $SE(2)$ and the dynamic effects related to single revolute joints in 2D cannot be extended to the case of multiple joints in 3D, see model in Sec. II-B. Moreover, in the 3D space, the propeller drag torques arise and have to be taken into account, see discussion in Sec. III-A.

We will now revise the main MAV designs proposed in the literature and show that none of them has all the four desirable properties described above.

Standard underactuated MAVs like quadrotors and hexarotors tick the Internal-force Property as they have all propellers fixedly oriented with spinning axes parallel to each other; however, because of the fixed attachment between the propellers and the body frame, their only hovering equilibria are characterized by the attitudes where the z axis is aligned with the gravity vector. Thus, they do not tick the Equilibria property.

Aerial vehicles equipped with the ability to hover while maintaining a larger set of orientations, known as fully-actuated MAVs, are surveyed in [7]. These MAVs cannot be stabilized at any pose but at a subset of poses in $SE(3)$ determined by the thrust limits, the design kinematics, and joint limits. Such subset contains any position but only a subset of all the orientations in general. A subclass of this type of MAVs, called omnidirectional MAV [8], can hover at any pose: namely, they have the Equilibria property mentioned above. These aerial vehicles can be divided in two classes.

The first class of designs that have been proposed to achieve full actuation or omnidirectionality are realized by fixedly tilting the propellers in such a way that their spinning axes are not all parallel to each other. As a consequence, all of these designs do not have the Internal-force Property. Examples are [9], a fully actuated hexarotor, and [10], [11], omnidirectional hexarotors. Other omnidirectional fixedly-tilted-propeller designs do not comply with the Input-

dimension Property, either; they are, for example, the heptarotor presented in [12] or the octarotors proposed in [13], [14].

The second design approach to achieve full-actuation or omnidirectionality while also partially achieving the Internal-force Property for at least some hovering orientations is the addition of servomotors that actively change the relative orientation between the propellers and the frame of the MAV. In [15], [16], the authors present a modification of the conventional quadrotor by actuating the tilt of each propeller separately via 4 servomotors for a total of 8 actuators. Similarly, in [17], the authors used 6 servomotors in addition to the 6 brushless motors that rotate the 6 propellers of an hexarotor. The design in [18] also falls in this category. They developed a MAV with multiple links connected in series by active revolute joints, with each link having two propellers that rotate simultaneously using a motor. In an attempt to limit the number of actuators, some designs have been proposed in which a single servo-motor is used to synchronously tilt all the propellers: 6 propellers are synchronously tilted by the additional actuator in [19], and 8 propellers in [20]. All the aforementioned designs do not comply with the Input-dimension Property, having a number of actuators greater than 6. Furthermore they do not comply with the Internal-force Property at any orientation but only some at some specific ones.

B. Contributions

The main contribution of this work is to propose the first MAV design, to the best of the authors’ knowledge, having the following four properties in $SE(3)$:

- 1) Input-dimension property. The number of actuators in the proposed MAV design is 6, equal to the number of DoFs of its base’s pose. There are 4 brushless motors, each making one propeller spin; 3 of the propellers are connected to a passive 2-DoF joint; one of the propeller’s attitude is actively controlled by 2 servomotors.
- 2) Equilibria property. In Proposition 1, we show that static hovering is feasible at *any* pose in $SE(3)$ of the MAV’s main body; in other words, a forced equilibrium exists for any base’s pose.
- 3) Internal-force property. Proposition 1 also shows that no internal forces are produced at the equilibrium for any base pose in $SE(3)$.
- 4) Stabilizability property. We prove in Theorem 1 that it is possible to create a state feedback law that renders the closed-loop system of the MAV asymptotically stable at any base pose in $SE(3)$, as long as configuration and thrust trajectories of the system remain in a certain neighborhood of that base pose. We observe that the dynamics of the passive propeller joints coincide with the zero dynamics, and we prove its asymptotical stability using the Lyapunov theory. The feedback control law is given in Proposition 2.

Eventually, simulation results of the closed-loop system in the presence of non-idealities, such as noise and parameter uncertainties, are presented, in order to provide an acceptable

level of confidence in the generalizability of the result beyond the standard model used to formally prove all the properties.

These properties capture major requirements for enabling *energy-efficient* omnidirectional flight. In particular, the ability to hover at any attitude in $SO(3)$ is the defining feature of omnidirectional MAVs [14], [15], hence expanding their reachable workspace and manipulation capabilities [12]. Ensuring stabilizability of these equilibria is essential for any practical deployment. Moreover, achieving full 6-DOF control with only 6 actuators alongside eliminating internal forces at hovering directly contributes to significantly improved energy efficiency, simplified input allocation, and extended flight endurance [13], [21], [22]. Together, these properties illustrate the impact of the proposed MAV concept within the field of aerial robotics.

C. Motivations Behind the Design Idea

The simplest MAV design that one could think of that respects the Input-dimension Property and the Internal-force Property (and potentially the Equilibria Property) is the one with 6 propellers, all free to passively tilt like 3D pendulums. However, the results achieved for the 2D example in [6] showed that a design with 3 passively linked propellers in a pendulum like fashion, in that case, was non-feedback linearizable as the allocation matrix was structurally rank-deficient at the static equilibria. Based on such a preliminary result, we discarded the all-passive-propeller design.

Hence, our design has servomotors that actively reorient one propeller. An alternative could be to reorient actively *all* the four propellers synchronously by means of the two servomotors and a transmission mechanism. However, the design of such a mechanism to drive the whole propeller joints synchronously is not trivial, would bring mechanical complexity and with it additional payload, cost, and maintenance effort; furthermore, it would not scale well with the size of the vehicle, when the motion needs to be transferred over longer distances. Instead, the proposed design where the servomotors exert their actuation locally at one individual propeller has the advantage of being modular and simple from a mechanical point of view, not posing challenges when increasing the dimensions of the vehicle.

D. Outline

The rest of the paper is organized as follows. Sec. II describes the dynamic model of the proposed novel MAV conceptual idea, whereas Sec. III identifies the equilibria sets of that model being all the poses in $SE(3)$ and all having the internal force property. Afterwards, we investigate and demonstrate that the system can be made asymptotically stable at all these equilibria by a state feedback in Sec. IV. Numerical simulations where the MAV performs decoupled motions are the subject of Sec. V. We conclude by giving some remarks on the future work in Sec. VI. For ease of exposition, all the formal proofs, derivations, and explicit calculation formulas are collected in appendices of [29].

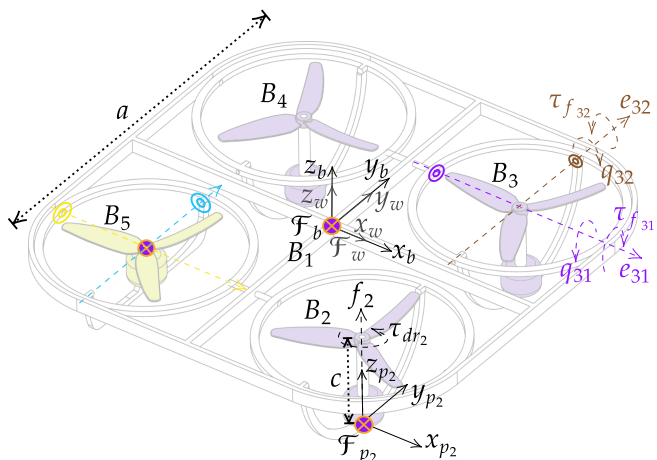


Fig. 1: Conceptual representation of the proposed MAV idea. The origins of the frames \mathcal{F}_b and \mathcal{F}_{p_2} are attached to CoMs of the base B_1 and the propeller link B_2 , respectively. The shown configuration is when \mathcal{F}_b coincides with \mathcal{F}_w and all the frames of the links have the same orientation as \mathcal{F}_w . The joint q_{j1} and q_{j2} positions are zero when \mathcal{F}_{p_j} has the same orientation as \mathcal{F}_b , $j = \{2, \dots, 5\}$. The link B_5 is attached to B_1 through an active joint, unlike the rest of the joints which are passive.

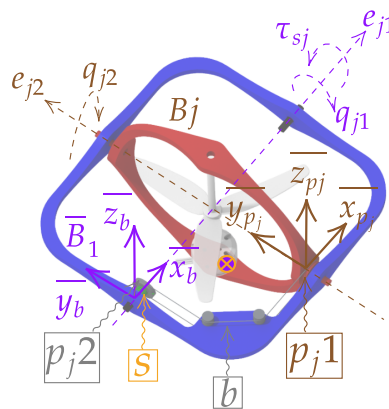


Fig. 2: The connection between B_j ($j = 2, 3, 4$) and the base B_1 in PJD_2 consists of universal passive joint with a Pulley-Belt-Spring module. B_j is the intermediate link connecting B_1 to B_j . b , p and s denote the belt, pulley and a torsion spring, respectively. τ_{sj} is the torsion spring torque around the rotation axis of q_{j1} , i.e. e_{j1} .

II. PROPOSED DESIGN AND DYNAMICAL MODEL

In this section, we describe the proposed design and present its dynamical model in state-space form.

A. Mechanical Design Idea

The vehicle concept, shown in Fig. 1, consists of a main rigid body, referred to as the *base* and denoted by B_1 , and four smaller bodies, referred to as *links* and denoted by B_2, B_3, B_4 , and B_5 . Each link carries a rigidly-attached motor driving a propeller and is connected to the base by two revolute joints. The propeller, the motor, the link, and the two revolute joints together form an *actuation unit*. For each unit, the joints' mutually-orthogonal rotation axes intersect at a point, called the *center of rotation* of the link, coinciding with the propeller center. The actuation units are mounted on

B_1 such that all centers of rotation lie on the same plane, resulting in a *coplanar design*. The centers of mass (CoMs) of B_2, B_3 , and B_4 are located below their respective centers of rotation, achieved by placing the motors sufficiently low. This makes these links behave as spatial pendula, with the joints acting as pivots. In contrast, B_5 's CoM coincides with its center of rotation. B_1 is connected to B_5 by an actuated universal joint with configuration $q_a = \text{col}(q_{5i}) \in \mathbb{T}^2$, and to B_2, B_3 , and B_4 by passive universal joints with configurations $q_p = \text{col}(q_{ji}) \in \mathbb{T}^6$, $j = 2, \dots, 5$, $i = 1, 2$.

For modeling simplicity, the actuated joint is assumed to be driven by fast velocity-controlled servo DC motors, neglecting motor dynamics. Moreover, B_5 's mass is assumed to be concentrated at its CoM, zeroing its angular inertia moment. Under these assumptions, the projected dynamics of B_5 onto its q_a 's screw axis vanish, rendering \dot{q}_a governed solely by the motor input.

Two Passive Joint Designs (PJD) are considered. In PJD₁, the passive joints are implemented as described above. In PJD₂, an additional Pulley-Belt-Spring module (Fig. 2) is integrated into each passive joint. This module transfers the rotation about q_{j2} 's axis to a rotation about q_{j1} 's axis through a belt-pulley transmission. A torsion spring, mounted along q_{j1} 's axis, applies a moment proportional to q_{j2} , thus the mechanism is unidirectional: rotations about q_{j2} generate a restoring moment about q_{j1} , while the reverse is not true. The rationale behind PJD₂ is discussed in Sec. III-A. Unless otherwise stated, the analysis herein applies to both designs.

B. Equations of Motion

We denote with $\mathcal{Q} = (C_1^0, q_p, q_a) \in SE(3) \times \mathbb{T}^8$ the system's configuration. The velocity of (C_1^0, q_p) is $(V_1^0, \dot{q}_p) \in \mathbb{R}^{12}$ where $[V_1^0] = \dot{C}_1^0(C_1^0)^{-1} \in se(3)$. Denote the full state vector $x(t)$ as $x = (C_1^0, q_p, V_1^0, \dot{q}_p, q_a)^T \in \mathbb{X} \equiv SE(3) \times \mathbb{T}^8 \times \mathbb{R}^{12}$. Dropping dependencies for clarity, the system dynamics is thus described by these state space equations

$$\Sigma_1 : \begin{cases} \dot{x} = F_1(x) + G_1(x)u \\ = \begin{pmatrix} [V_1^0] C_1^0 \\ \dot{q}_p \\ M^{-1}(-h - g + \bar{\tau}_f) \\ 0_{2 \times 1} \end{pmatrix} + \begin{pmatrix} 0_{12 \times 6} \\ D_b \quad 0_{6 \times 2} \\ D_p \quad 0_{6 \times 3} \\ 0_{2 \times 4} \quad I_{2 \times 2} \end{pmatrix} u \end{cases} \quad (1)$$

where explicit formulas of M, h and g are given in Sec. A [29], and D_b, D_p and the input vector u are defined as

$$D_b = \begin{pmatrix} \text{Ad}_{(C_{f_2}^0)^{-1}} \bar{f}_2 & \text{Ad}_{(C_{f_3}^0)^{-1}} \bar{f}_3 & \text{Ad}_{(C_{f_4}^0)^{-1}} \bar{f}_4 & \text{Ad}_{(C_{f_5}^0)^{-1}} \bar{f}_5 \end{pmatrix}_{6 \times 4}$$

$$D_p = \begin{pmatrix} S_2^T \text{Ad}_{(C_{f_2}^0)^{-1}} \bar{f}_2 & 0 & 0 \\ 0 & S_3^T \text{Ad}_{(C_{f_3}^0)^{-1}} \bar{f}_3 & 0 \\ 0 & 0 & S_4^T \text{Ad}_{(C_{f_4}^0)^{-1}} \bar{f}_4 \end{pmatrix}_{6 \times 3}$$

$$u = (f_2 \quad f_3 \quad f_4 \quad f_5 \quad u_{v_1} \quad u_{v_2})_{6 \times 1}^T \in \mathbb{R}^6$$

where $f = \text{col}(f_i)$ and f_i is the thrust magnitude of the propeller attached to B_i , with $i = 2, \dots, 5$; \bar{f}_i is a constant vector given as $\bar{f}_i := (0 \ 0 \ k_i \ 0 \ 0 \ 1)_{6 \times 1}^T$. u_v is tilting speed. $C_{f_i}^0 \in SE(3)$ is the homogeneous transformation of a frame \mathcal{F}_{f_i} attached at the propeller of link B_i relative to the inertial frame \mathcal{F}_w .

Result 1 (Input dimension property). *The proposed design satisfies the input dimension property. In fact the dimension of the manifold of the configuration of the base frame C_1^0 is six and the dimension of the input is $\dim(u) = 6$ (four propeller thrusts and two servomotor speeds).*

III. STUDY OF ATTAINABLE EQUILIBRIA AND INTERNAL FORCES AT EACH EQUILIBRIUM

In this section we obtain the set of forced equilibria of the dynamics (1) and investigate their properties in terms of the corresponding four thrust forces produced at these configurations. We begin by giving some preliminary definitions. Afterwards, the main result, which establishes the Equilibria property and the Internal-force property, is summarized in Proposition 1 whose proof is found in Sec. D of [29].

Imposing $\dot{x}(t) = 0$ in (1) implies $(V_1^0, \dot{q}_p, \dot{q}_a) = 0$, which defines an equilibrium condition at which the state and the input become, respectively, $x_e = (C_{1e}^0, q_{pe}, 0, 0, q_{ae})^T$ and $u_e = (f_e \ u_{ve})^T$, with $f_e = (f_{2e} \ f_{3e} \ f_{4e} \ f_{5e})^T$ and $u_{ve} = (u_{v_{1e}} \ u_{v_{2e}})^T$. Under this condition, both $h(C_1^0, q_p, V_1^0, \dot{q}_p) = 0$ and $\bar{\tau}_f(\dot{q}_p) = 0$ vanish, as they depend quadratically and linearly, respectively, on the configuration velocity.

For PJD₁, (1) reduces to this static balance vector equation whose admissible solutions are the equilibrium state and input pairs (x_e, u_e) such that

$$g_b(C_{1e}^0, q_{pe}) = (D_b \ 0_{6 \times 2}) u_e,$$

$$g_p(C_{1e}^0, q_{pe}) = (D_p \ 0_{6 \times 3}) u_e$$

$$= (\tau_{d2} \ 0 \ \tau_{d3} \ 0 \ \tau_{d4} \ 0)_{6 \times 1}^T$$

$$0_2 = u_{ve} \quad (2)$$

where $\tau_{dj} = k_j f_{je} \sin(q_{j2e})$, with $j = 2, 3, 4$. C_{1e}^0 and $q_{pe} = \text{col}(q_{je})$, with $q_{je} = \text{col}(q_{jie}) \ \forall j = 2, 3, 4, \forall i = 1, 2$.

A. Effect of the Aerodynamic Drag Torque at the Equilibrium

The presence of the torque τ_{dj} in (2) leads to the important consequence that the value of the joints q_{pe} at the equilibrium is not solely determined by the gravitational torque at equilibrium g_{pe} , as it is the case for the 2D MAV presented in [6], but also by a component of the equilibrium thrust f_e at equilibrium.

This residual torque τ_{dj} can be eliminated at any equilibrium by the spring introduced in PJD₂ whose proposed implementation in Fig. 2 enables a torsion spring to counteract residual torque and passively return the link to its vertical configuration, zeroing the internal force as stated in proposition 1. In fact, we can tune each variable-stiffness torsion spring such that its stiffness $k_s = \frac{\partial \tau_{sj}}{\partial q_{j2}}$ varies linearly with $\cos(q_{j2})$, with a constant slope $\bar{k} = k_j f_{je}$, i.e. $k_s = \bar{k} \cos(q_{j2})$, which is feasible since f_{je} is found to be constant for any equilibrium of PJD₂ as long as the vehicle weight remains constant during flight as shown in Sec. D of [29]. Hence, the spring needs not to change or be re-tuned between flights. As a result, this component τ_{dj} is canceled at any PJD₂ equilibrium, i.e. when $\tau_{dj} = -\tau_{sje}$, transforming (2) to

$$g_p(C_{1e}^0, q_{pe}) = 0_6, \quad u_{ve} = 0_2. \quad (3)$$

B. Minimal Thrust at Equilibrium vs Presence of Internal Forces

Before presenting the result on the Equilibria and Internal-force properties of the proposed MAV (1) we provide two definition for the thrust magnitudes at the equilibrium, in the case in which they are minimal and in the case in which there is internal force.

Definition 1. A vector of thrust magnitudes $f \in \mathbb{R}_{\geq 0}^l$, where $\mathbb{R}_{\geq 0}^l := \{s = \text{col}(s_i) \in \mathbb{R}^l \mid s_i \geq 0, \forall i \in \{1, \dots, l\}\}$, is said to be minimal at the equilibrium if it belongs to $\mathcal{F}_{\min}^{\text{eq}}$, defined as:

$$\mathcal{F}_{\min}^{\text{eq}} := \left\{ f = \text{col}(f_i) \in \mathbb{R}_{\geq 0}^l \mid \sum_{i=1}^l f_i = m_{\text{tot}} g_r \right\} \quad (4)$$

where m_{tot} is the robot's mass and $g_r = 9.81 \text{ m/s}^2$. Instead, f is said to have internal forces at the equilibrium if it belongs to $\mathcal{F}_{\text{int.for.}}^{\text{eq}}$, defined as:

$$\mathcal{F}_{\text{int.for.}}^{\text{eq}} := \left\{ f = \text{col}(f_i) \in \mathbb{R}_{\geq 0}^l \mid \sum_{i=1}^l f_i > m_{\text{tot}} g_r \right\}$$

A MAV design whose thrust magnitudes are minimal at all its equilibria is said to have no internal forces at its equilibria.

In other words, a minimal thrust magnitudes vector $f_e \in \mathcal{F}_{\min}^{\text{eq}}$ has the least amount of total thrust magnitudes necessary to counteract the gravity at the equilibrium, whereas $f_e \in \mathcal{F}_{\text{int.for.}}^{\text{eq}}$ means that the vehicle generates more total thrust than what is strictly necessary for compensating gravity, thus having some wasted internal force. Moreover, there exists a unique orientation for each propeller in an MAV such that when all the propellers assume such orientation the absence of internal force is guaranteed at hovering, proven in Lemma 1 in Sec. C [29]. The following proposition establishes the main result of this section.

Proposition 1. Consider any pose for the base B_1 denoted by C_{1e}^0 . Then the following statements hold true and are equivalent for the system (1):

- 1) For any base pose $C_{1e}^0 \in SE(3)$, there exists an equilibrium for PJD₂ in which the joint equilibrium configuration $q_{pe}^{[2]}$ satisfies $C_j^0(C_{1e}^0, q_{je}^{[2]})e_3 = e_3 \forall j \in \{2, \dots, 5\}$ and a thrust magnitudes vector $f_e^{[2]} \in \mathcal{F}_{\min}^{\text{eq}}$ is produced whose elements $f_{je}^{[2]} = g_r(\frac{1}{4}m_b + m_j)$ are constants $\forall C_{1e}^0$ with k_i chosen by $\sum_{j=2}^5 k_i(\frac{1}{4}m_b + m_j) = 0$.
- 2) For any base pose C_{1e}^0 , PJD₂ has no internal force at any equilibrium $q_{pe}^{[2]}$, by Definition 1, as a corollary of $f_e^{[2]} \in \mathcal{F}_{\min}^{\text{eq}}$ (Statement 1).
- 3) When $\tau_{dj} \neq 0$, PJD₁ has no joint equilibrium $q_{pe}^{[1]}$ in which each propeller produces a minimal thrust: $C_j^0(C_{1e}^0, q_{je}^{[1]})e_3 \neq e_3, \forall \tau_{dj} \neq 0$.
- 4) When $\tau_{dj} \neq 0$, it follows from Statement 3, and Lemma 1 in [29], that PJD₁ has an internal force $f_e^{[1]} \in \mathcal{F}_{\text{int.for.}}^{\text{eq}}$. The amount of such force can be reduced by changing parameters k_i, c and m_j .

Proof. See Sec. D of [29]. \square

The state equilibria set for PJD_i is denoted by $\mathbb{D}_{x_e}^{[i]}$ whereas $\mathbb{D}_{f_e}^{[i]}$ signifies their associated thrust equilibrium sets. The explicit relations are given in Sec. D.4 [29].

We conclude the section remarking that the perfect vertical alignment of propellers in any PJD₂ equilibrium is possible thanks to each spring torque τ_{sje} absorbing the residual drag τ_{dj} affecting the joint variable q_{j1} . This allows any joint equilibrium $q_{pe}^{[2]}$ to be dictated only by the gravity acting on the CoMs of the pendulum-like links B₂-B₄, given that the pivots, i.e., the joints, are passive.

Remark 1. The design using PJD₁ constitutes still an excellent compromise between mechanical simplicity and energy efficiency, with the ability to outperform the state of the art designs when it comes to the amount of internal force needed at the the equilibria. In fact, for typical values of the aerodynamic and kinematic parameters, the difference in the amount of internal forces generated in PJD₁ design remains significantly small compared to the ideal PJD₂ case, as it can be seen for example in the simulations of Section V. This supports the viability of the concept from a mechanical perspective by using the simpler design PJD₁, if one does not want to resort to the particular joint design in PJD₂.

IV. STABILIZATION OF THE EQUILIBRIA

Following the characterization of the Equilibria and Internal-Force properties in Proposition 1, this section presents the solution of the problem of whether every equilibrium point in the equilibria set $\mathbb{D}_{x_e}^{[i]}$ can be made closed-loop asymptotically stable, at least locally, by a regular state feedback law, hence establishing the Stabilizability property. The core findings are stated in Theorem 1 and Proposition 2. The proposed control architecture is shown in Fig. 3.

The analysis departs by noticing that there exists no static state feedback control law rendering the closed-loop system Σ_1 in (1) locally asymptotically stable (LAS) in an open neighborhood $\mathbb{U}_{x_e} \subseteq \mathbb{X}$ of an equilibrium $x_e \in \mathbb{D}_{x_e}^{[i]}$, since it turns out that Σ_1 does not possess a well-defined vector relative degree at any $x_e \in \mathbb{D}_{x_e}^{[i]}$ [23]. However, the goal of stabilizing this closed-loop system at x_e remains attainable by a dynamic state feedback obtained from the dynamic extension algorithm [24], as illustrated in Theorem 1.

Theorem 1. Let the original system Σ_1 (1) be decomposed into Σ_2 and Σ_3 , respectively given by $\Sigma_3 : \dot{C}_1^0 = [V_1^0] C_1^0$ and this Σ_2

$$\Sigma_2 : \begin{cases} \dot{x}_2 = F_2(x) + G_2(x)u \\ = \begin{pmatrix} \dot{q}_p \\ M^{-1}(-h - g + \bar{\tau}_f) \\ 0_{2 \times 1} \end{pmatrix} + \begin{pmatrix} 0_{6 \times 6} & \\ D_b & 0_{6 \times 2} \\ D_t & 0_{6 \times 3} \\ 0_{2 \times 4} & I_{2 \times 2} \end{pmatrix} u \end{cases} \quad (5)$$

Then, these statements are true:

- 1) Σ_2 is dynamically input/output feedback linearizable w.r.t the I/O pair (u, h_y) , where the output function $h_y(t) : t \rightarrow \mathbb{R}^6$ is $h_y(t) = V_1^0$, by a dynamic

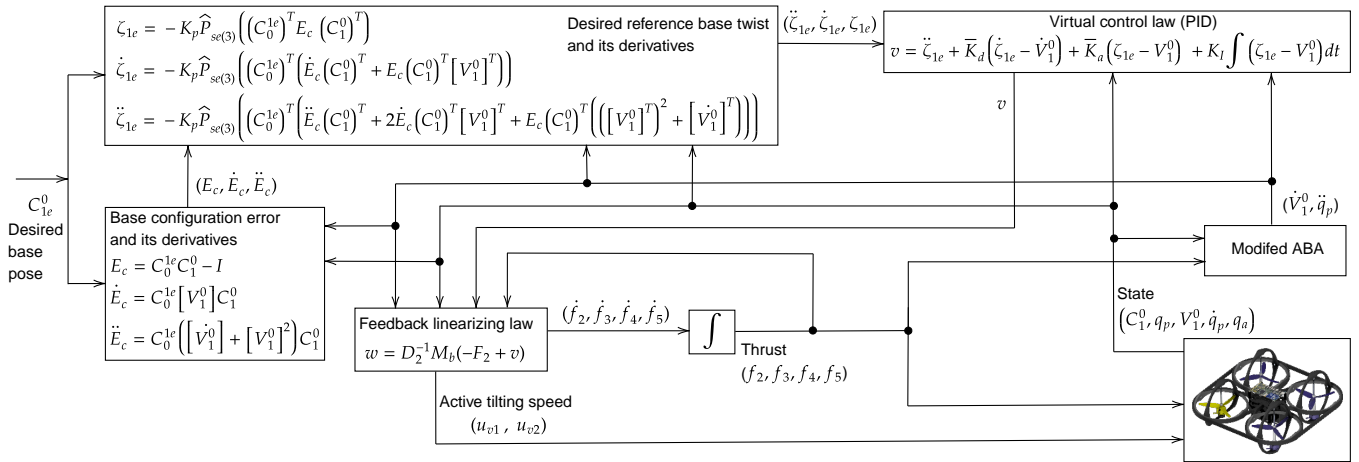


Fig. 3: Block diagram of the proposed control scheme. It takes a desired base pose $C_{1e}^0 \in SE(3)$ and converts it into a reference base twist $\zeta_{1e}(t)$ through configuration error feedback E_c . Dynamic FBL is applied to the twist dynamics, which are stabilized using a PID controller. The accelerations are efficiently computed via a modified Articulated-Body Inertia Algorithm (ABA) in Sec. B of [29].

extension [24] given by this input precompensator

$$z(t) = \text{col}(z_i) := f(t) \in \mathbb{R}^4, \dot{z} = \bar{w} \in \mathbb{R}^4, i = 2, \dots, 5. \quad (6)$$

The extended state is $\bar{x} = (q_p, V_1^0, \dot{q}_p, q_a, z) \in \bar{\mathbb{X}} \equiv \mathbb{T}^8 \times \mathbb{R}^{16}$ whereas the linearizing state feedback on the extended system, whose I/O pair is (w, h_y) , is given by

$$w = \begin{pmatrix} \bar{w} \\ u_{v1} \\ u_{v2} \end{pmatrix} = D_2^{-1} M_b(-E_2 + v) \quad (7)$$

where $v \in \mathbb{R}^6$ is the virtual input, and E_2, D_2 and M_b are given in (31), (27) and (30) of Sec. E [29]. This dynamic FBL is well-defined in an open neighborhood $\mathbb{U}_{\bar{x}_e} \subseteq \bar{\mathbb{X}}$ of $\bar{x}_e \in \mathbb{D}_{\bar{x}_e}^{[z]} \cup \mathbb{D}_{f_e}^{[z]}$ defined as

$$\mathbb{U}_{\bar{x}_e} = \left\{ \bar{x}(t) \in \bar{\mathbb{X}} \mid \det(D_2(\bar{x})) \neq 0 \right\}$$

- 2) For any base pose $C_{1e}^0 \in SE(3)$, The original system Σ_1 , extended with the precompensator (6), has locally, in $\mathbb{U}_{\bar{x}_e} \times SE(3)$, asymptotically stable (LAS) zero dynamics w.r.t the output h_y , iff $\forall \bar{x} \in \mathbb{Z}_x - \{\bar{x}_e\}$

$$\|\tilde{f}\| < \frac{1}{\|D_3(q_p - q_{pe})\|} \lambda_{\min}(D_f) \|\dot{q}_p\| \quad (8)$$

where $\tilde{f} = \text{col}(f_i), i = 2, 3, 4, \mathbb{Z}_x$ and D_3 are respectively given in (38) and (34) in [29]. $D_f > 0 \in \mathbb{R}^{6 \times 6}$ contains the constant passive joints friction coefficients.

Proof. See Sec. E in [29]. \square

This means that, as long as the extended system trajectories remain in $\mathbb{U}_{\bar{x}_e} \times SE(3)$ where the decoupling holds, any base pose C_{1e}^0 of the original system Σ_1 (1) can be made locally asymptotically stable by a dynamic state feedback. Proposition 2 constructs the the virtual controller that stabilizes the resulting linearized twist dynamics.

Proposition 2. Consider the virtual control input v given by

$$v = \ddot{\zeta}_{1e} + \bar{K}_d(\dot{\zeta}_{1e} - \dot{V}_1^0) + \bar{K}_a(\zeta_{1e} - V_1^0) \quad (9)$$

where $\zeta_{1e}, \dot{\zeta}_{1e}, \ddot{\zeta}_{1e} \in \mathbb{R}^6$ are respectively given in (43) and (46) [29] and shown in Fig. 3. \bar{K}_d and $\bar{K}_a \in \mathbb{R}^{6 \times 6}$ are positive definite diagonal gain matrices chosen such that to make $(A - BK)$ Hurwitz where

$$A = \begin{pmatrix} 0_{6 \times 6} & I_{6 \times 6} \\ 0_{6 \times 6} & 0_{6 \times 6} \end{pmatrix}, B = \begin{pmatrix} 0_{6 \times 6} \\ I_{6 \times 6} \end{pmatrix}, K = \begin{pmatrix} \bar{K}_a & \bar{K}_d \end{pmatrix}$$

Given the precompensator in (6) and the linearizing control law in (7), substituting v into (7) asymptotically stabilizes the extended system Σ_1 with (6) in the open neighborhood $\mathbb{U}_{\bar{x}_e} \times SE(3)$.

Proof. See Sec. F in [29]. \square

We note that the system (1) evolves on the product Lie group $SE(3) \times \mathbb{T}^8$ due to the internal joint dynamics. This motivates our use of the normal-form approach [27], as it facilitates the study of the associated zero dynamics. Although the proposed controller, shown in Fig. 3, employs tools often considered coordinate-dependent, the Lie-group formulation guarantees that the control laws are coordinate-invariant, i.e. their validity does not depend on a specific local parameterization of the configuration $SE(3) \times \mathbb{T}^8$.

V. SIMULATION TESTS

This section reports high-fidelity Gazebo simulations, implemented via the GenoM3 framework, validating the proposed controller beyond the nominal model and under more realistic conditions such as presence of parametric uncertainty. For both designs PJD₁ and PJD₂, the controller (7), (9) with the dynamic extension (6), shown in Fig. 3, achieves independent stabilization of the MAV attitude and position. Two indicative desired base poses are considered: an attitude command of a 60° step in roll, pitch and yaw at fixed position, and a 1 [m] position step along the inertial (x, y, z) with constant orientation. The resulting trajectories are shown in Fig. 4. Simulation videos and plots for several different maneuvers are available at <https://youtu.be/SWIt0CSwNUo>. As noted from these simulations, the

vehicle can achieve a wide range of maneuvers while generating only positive thrust, potentially reducing the complexity associated with the use of bidirectional propellers. The state and input evolutions exhibit some oscillations due to the imperfections introduced by large parametric uncertainty and actuator noise from the emulated hardware.

The simulations use $m_b = 1$, $m_j = 0.479$, $m_5 = 0.12$ kg, with B_j 's inertias ($\text{kg}\cdot\text{m}^2$) $I_{px} = I_{py} = 2.18 \times 10^{-3}$, $I_{pz} = 1.17 \times 10^{-6}$, and B_1 's inertias $I_{bx} = I_{by} = 8.33 \times 10^{-3}$ and $I_{bz} = 1.67 \times 10^{-2}$. The distance (m) between adjacent joints is $a = 0.2$ whereas from each joint to the corresponding link CoM is $c = 0.16$. Friction coefficients are $b_{f_{j1}} = b_{f_{j2}} = 0.05$ N·m/s/rad, and the k_j ratio is 0.01. These values are each perturbed by +10%. The gains $\bar{K}d = \text{diag}(5.55)$ and $\bar{K}a = \text{diag}(14.94)$ are obtained via LQR applied to the system in Prop 2, using weighting matrices $W_x = \text{diag}(0.0001) \in \mathbb{R}^{12 \times 12}$ and $W_u = \text{diag}(0.0001) \in \mathbb{R}^{6 \times 6}$. The gain $K_I = \text{diag}(30)$ is tuned empirically to eliminate steady-state error. The gain $K_p = \text{diag}(0.1)$ in (43) [29] regulates the convergence rate of C_1^0 to C_{1e}^0 , hence the evolution speed of the reference trajectory ζ_{1e} . For fixed \bar{K}_d and \bar{K}_a , increasing K_p leads to larger transient errors, requiring higher thrust and faster tilting for q_a .

To illustrate the stability of the zero dynamics (39) [29], as proven in Sec. E, we simulated its evolution under nominal conditions with initial values $C_1^0(0) = I_{4 \times 4}$, $q_p(0) = -30^\circ \times \mathbf{1}_{6 \times 1}$, $\dot{q}_p(0) = 0.1 \times \mathbf{1}_{6 \times 1}$ rad/s. As shown in Fig. 5, the q_p and \dot{q}_p converge to zero, confirming convergence to the equilibrium q_{pe} corresponding to that base pose $C_{1e}^0(0)$.

We conclude by comparing PJD₁ and PJD₂ in terms of the total equilibrium thrust for a scenario where a step command of 60° in pitch is given. As plotted in Fig. 6, the equilibrium thrust of PJD₁ satisfies $\sum_{j=2}^5 f_{je}^{[1]} = 1.02 \sum_{j=2}^5 f_{je}^{[2]}$ with $f_e^{[2]} = f_{min} \in \mathcal{F}_{min}^{\text{eq}}$, i.e. a 2% increase over the minimal thrust $f_e^{[2]}$ in PJD₂, since the desired pose C_{1e}^0 requires residual torque $\tau_{dj} \neq 0$, leading to $q_{pe}^{[1]} \neq q_{pe}^{[2]}$, i.e. not pointing upward. This confirms Prop 1.

VI. CONCLUSION

This work proposes a novel omnidirectional MAV concept enabling full 6-DoF motion with a minimum number of actuators and no internal forces at equilibrium. The design combines a rigid base evolving on $SE(3)$, thus avoiding representation singularities, with 4 propeller-carrying links connected through universal joints, 3 of which are passive whereas 1 is actively driven by 2 servomotors. We proved that the proposed MAV satisfies the Input-Dimension, Equilibria, Internal-Force, and Stabilizability properties. Without overactuation, an equilibrium exists for any base pose, and when torsion springs are employed, the total thrust exactly balances the vehicle weight. Even without springs, internal forces can be made arbitrarily small through changing the links masses and lengths. Any base pose can be rendered locally asymptotically stable via a dynamic FBL and backstepping from base pose error on $SE(3)$. High-fidelity sim-

ulations demonstrate decoupled position and attitude control under realistic conditions.

A possible mechanical implementation is illustrated in Fig. 7. This design scales favorably, as hovering loads are distributed almost evenly among propellers, avoiding excessive stress on the actively tilting unit. Scaling challenges are therefore typical to those of multirotors, such as propeller and battery sizing, rather than limitations specific to the proposed MAV.

Future work will focus on fully geometric control formulations on $SE(3) \times \mathbb{T}^8$, exploiting the passive-joint dynamics to construct a passivity-based controller, investigating a more generic propeller placements, extending the scheme to handle trajectory tracking, and carrying out experimental validation.

REFERENCES

- [1] M. Sabour, P. Jafary, and S. Nematian, "Applications and classifications of unmanned aerial vehicles: A literature review with focus on multi-rotors," *The Aeronautical Journal*, vol. 127, no. 1309, pp. 466–490, 2023.
- [2] G. Muscio, F. Pierri, M. A. Trujillo, E. Cataldi, G. Antonelli, F. Caccavale, A. Viguria, S. Chiaverini, and A. Ollero, "Coordinated control of aerial robotic manipulators: Theory and experiments," *IEEE Transactions on Control Systems Technology*, vol. 26, no. 4, pp. 1406–1413, 2017.
- [3] A. Ollero, M. Tognon, A. Suarez, D. Lee, and A. Franchi, "Past, present, and future of aerial robotic manipulators," *IEEE Transactions on Robotics*, vol. 38, no. 1, pp. 626–645, 2022.
- [4] M. Tognon, H. A. T. Chávez, E. Gasparin, Q. Sablé, D. Bicego, A. Mallet, M. Lany, G. Santi, B. Revaz, J. Cortés, and A. Franchi, "A truly-redundant aerial manipulator system with application to push-and-slide inspection in industrial plants," *IEEE Robotics and Automation Letters*, vol. 4, no. 2, pp. 1846–1851, 2019.
- [5] K. Bodie, M. Brunner, M. Pantic, S. Walser, P. Pfändler, U. Angst, R. Siegwart, and J. Nieto, "Active interaction force control for contact-based inspection with a fully actuated aerial vehicle," *IEEE Transactions on Robotics*, vol. 37, no. 3, pp. 709–722, 2021.
- [6] A. Ali, C. Gabellieri, and A. Franchi, "A control theoretic study on omnidirectional mavs with minimum number of actuators and no internal forces at any orientation," in *2024 IEEE 63rd Conference on Decision and Control (CDC)*, 2024, pp. 3571–3576.
- [7] R. Rashad, J. Goerres, R. Aarts, J. B. C. Engelen, and S. Stramigioli, "Fully actuated multirotor UAVs: A literature review," *IEEE Robotics & Automation Magazine*, vol. 27, no. 3, pp. 97–107, 2020.
- [8] M. Hamandi, Q. Sable, M. Tognon, and A. Franchi, "Understanding the omnidirectional capability of a generic multi-rotor aerial vehicle," in *2021 Aerial Robotic Systems Physically Interacting with the Environment (AIRPHARO)*, 2021, pp. 1–6.
- [9] S. Rajappa, M. Ryll, H. H. Bühlhoff, and A. Franchi, "Modeling, control and design optimization for a fully-actuated hexarotor aerial vehicle with tilted propellers," in *2015 IEEE International Conference on Robotics and Automation (ICRA)*, 2015, pp. 4006–4013.
- [10] T. D. Howard, C. Molter, C. D. Seely, and J. Yee, "The lynchpin—a novel geometry for modular, tangential, omnidirectional flight," *SAE International Journal of Aerospace*, vol. 16, no. 3, pp. 291–303, mar 2023. [Online]. Available: <https://doi.org/10.4271/01-16-03-0018>
- [11] S. Park, J. Her, J. Kim, and D. Lee, "Design, modeling and control of omni-directional aerial robot," in *2016 IEEE/RSJ International Conference on Intelligent Robots and Systems (IROS)*, 2016, pp. 1570–1575.
- [12] M. Hamandi, Q. Sable, M. Tognon, and A. Franchi, "Understanding the omnidirectional capability of a generic multi-rotor aerial vehicle," in *2021 Aerial Robotic Systems Physically Interacting with the Environment (AIRPHARO)*. IEEE, 2021, pp. 1–6.
- [13] D. Brescianini and R. D'Andrea, "Design, modeling and control of an omni-directional aerial vehicle," in *2016 IEEE International Conference on Robotics and Automation (ICRA)*, 2016, pp. 3261–3266.

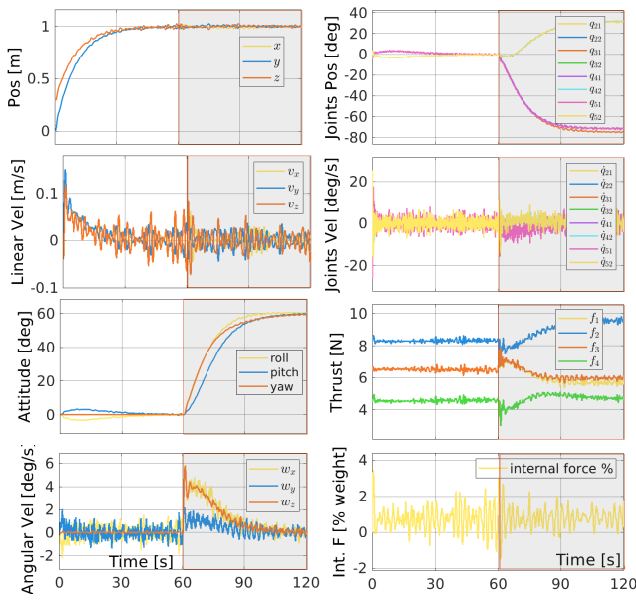
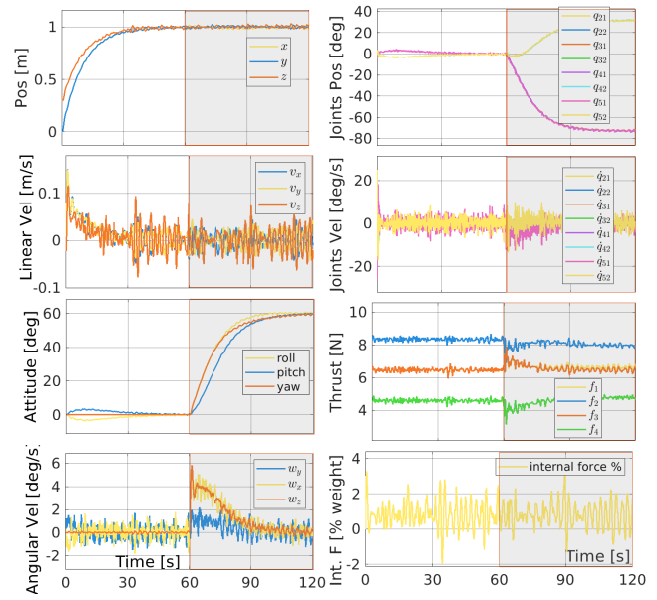
(a) PJD₁(b) PJD₂

Fig. 4: Evolutions of the state and input for (a) PJD₁ and (b) PJD₂ designs. The simulation has two phases: First (0-60s) is the position step with the initial attitude held constant. Second (60-120s, gray-shaded), the attitude step with the position at $t = 60$ s held constant.

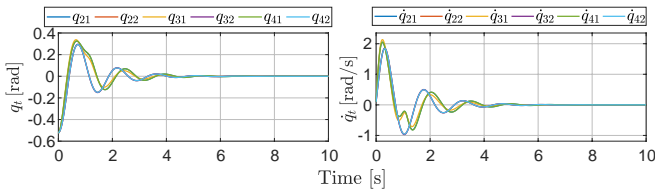


Fig. 5: zero dynamics evolution showing convergence.

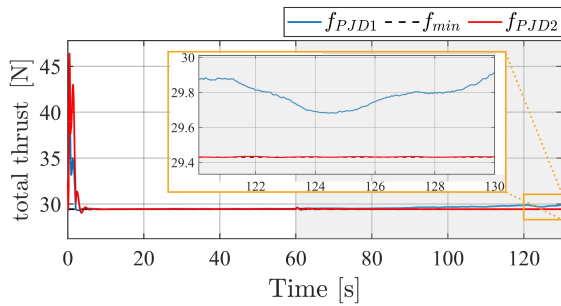


Fig. 6: Comparison of the total thrust between PJD₁ and PJD₂ when stabilizing a 60° pitch attitude step. In hovering, $\sum f_e^{[1]}$ is 2% higher than $\sum f_e^{[2]}$.

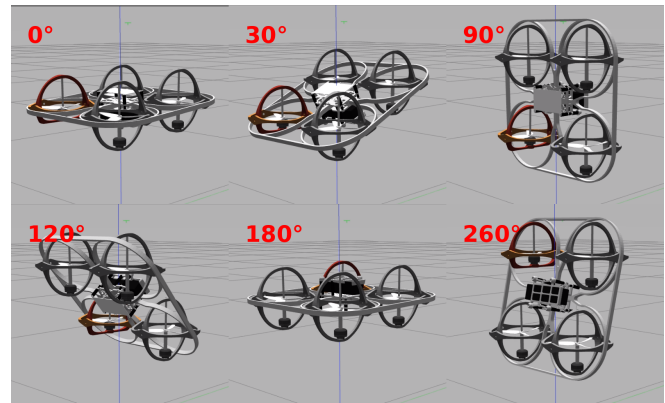


Fig. 7: The vehicle in Fig. 1. performing 260 degrees roll.

[14] S. Park, J. Lee, J. Ahn, M. Kim, J. Her, G.-H. Yang, and D. Lee, “Odar: Aerial manipulation platform enabling omnidirectional wrench generation,” *IEEE/ASME Transactions on mechatronics*, vol. 23, no. 4, pp. 1907–1918, 2018.

[15] M. Ryll, H. H. Bühlhoff, and P. R. Giordano, “A novel overactuated quadrotor unmanned aerial vehicle: Modeling, control, and experimental validation,” *IEEE Transactions on Control Systems Technology*, vol. 23, no. 2, pp. 540–556, 2014.

[16] A. Oosedo, S. Abiko, S. Narasaki, A. Kuno, A. Konno, and M. Uchiyama, “Flight control systems of a quad tilt rotor unmanned aerial vehicle for a large attitude change,” in *2015 IEEE International Conference on Robotics and Automation (ICRA)*, 2015, pp. 2326–2331.

[17] M. Kamel, S. Verling, O. Elkhatib, C. Sprecher, P. Wulkop, Z. Taylor, R. Siegwart, and I. Gilitschenski, “The voliro omniorientational hexa-

copter: An agile and maneuverable tilttable-rotor aerial vehicle,” *IEEE Robotics & Automation Magazine*, vol. 25, no. 4, pp. 34–44, 2018.

[18] M. Zhao, T. Anzai, F. Shi, X. Chen, K. Okada, and M. Inaba, “Design, modeling, and control of an aerial robot dragon: A dual-rotor-embedded multilink robot with the ability of multi-degree-of-freedom aerial transformation,” *IEEE Robotics and Automation Letters*, vol. 3, no. 2, pp. 1176–1183, 2018.

[19] M. Ryll, D. Bicego, and A. Franchi, “Modeling and control of fast-hex: A fully-actuated by synchronized-tilting hexarotor,” in *2016 IEEE/RSJ International Conference on Intelligent Robots and Systems (IROS)*, 2016, pp. 1689–1694.

[20] Y. Aboudorra, C. Gabellieri, R. Brantjes, Q. Sablé, and A. Franchi, “Modelling, analysis, and control of omnimorph: an omnidirectional morphing multi-rotor uav,” *Journal of Intelligent & Robotic Systems*, vol. 110, no. 1, p. 21, 2024.

[21] K. Bodie, Z. Taylor, M. Kamel, and R. Siegwart, “Towards efficient full pose omnidirectionality with overactuated MAVs,” in *Proc. Int. Symp. Experimental Robotics*, J. Xiao, T. Kröger, and O. Khatib, Eds. Cham: Springer, 2020, pp. 85–95.

[22] M. Hamandi, F. Usai, Q. Sablé, N. Staub, M. Tognon, and A. Franchi, “Design of multirotor aerial vehicles: a taxonomy based on input allocation,” *The International Journal of Robotics Research*, vol. 40, no. 8-9, pp. 1015–1044, 2021.

[23] A. Isidori, *Nonlinear Control Systems II*, ser. Communications and

Control Engineering. Springer London, 1999. [Online]. Available: <https://link.springer.com/book/10.1007/978-1-4471-0549-7>

- [24] J. Descusse and C. Moog, "Dynamic decoupling for right-invertible nonlinear systems," *Systems & Control Letters*, vol. 8, no. 4, pp. 345–349, 1987. [Online]. Available: <https://www.sciencedirect.com/science/article/pii/0167691187901010>
- [25] R. Featherstone, *Rigid body dynamics algorithms*. Springer, 2014.
- [26] R. M. Murray, Z. Li, and S. S. Sastry, *A mathematical introduction to robotic manipulation*. CRC press, 2017.
- [27] A. Isidori, *Nonlinear Control Systems*, ser. Communications and Control Engineering. Springer London, 2013. [Online]. Available: <https://books.google.it/books?id=N9h5BgAAQBAJ>
- [28] M. Spong, "Partial feedback linearization of underactuated mechanical systems," in *Proceedings of IEEE/RSJ International Conference on Intelligent Robots and Systems (IROS'94)*, vol. 1, 1994, pp. 314–321 vol.1.
- [29] A. Ali, C. Gabellieri, and A. Franchi, "Exploring a new design paradigm for omnidirectional MAVs for minimal actuation and internal force elimination: Theoretical framework and control," *arXiv preprint arXiv:2510.15071*, 2025.

APPENDIX

A. Explicit Expressions of dynamical model

In this subsection, we collect the definitions and analytical expressions of the variables appearing in the system dynamics (1). In the following, $j = 2, 3, 4$ and $i = 1, 2$.

a) Mass matrix: The generalized mass matrix of the system is

$$M = \begin{pmatrix} M_{bb} & M_{bp} \\ M_{bp}^T & M_{pp} \end{pmatrix}.$$

The base inertia block is

$$M_{bb} = M_{B_1}^0 + \sum_{j=2}^5 M_{B_j}^0,$$

where $M_{B_j}^0$ denotes the inertia tensor of body B_j expressed in the world frame \mathcal{F}_w . The coupling M_{bp} and joint inertia matrices M_{pp} are respectively defined as

$$M_{bp} = \sum_{j=2}^4 M_{B_j}^0 S_j, \quad M_{pp} = \text{blkdiag}(S_j^T M_{B_j}^0 S_j).$$

b) Time derivatives: The time derivative of the inertia tensor of body B_j expressed in \mathcal{F}_w is obtained from

$$\dot{M}_{B_j}^0 = -M_{B_j}^0 \text{ad}_{V_j^0} - \text{ad}_{V_j^0}^T M_{B_j}^0,$$

where $\text{ad}_{(\cdot)}$ denotes the Lie-algebra adjoint operator and

$$V_j^0 = V_1^0 + S_j \dot{q}_j, \quad j \in \{2, 3, 4\}.$$

For $j = 5$, one has

$$\dot{M}_5^0 = -M_5^0 \text{ad}_{V_1^0} - \text{ad}_{V_1^0}^T M_5^0.$$

The time derivative of the joint screw is given by

$$\dot{S}_j = \text{ad}_{V_j^0} S_j.$$

c) Coriolis and centrifugal terms: The Coriolis and centrifugal vector is defined as

$$h = (h_b \quad \text{col}(h_j))^T.$$

The base component h_b is computed from

$$h_b = \dot{M}_{bb} V_1^0 + \sum_{j=2}^4 (M_{B_j}^0 \dot{S}_j + \dot{M}_{B_j}^0 S_j) \dot{q}_j,$$

while the B_j 's Coriolis & centrifugal terms projected onto the corresponding joint J_{1j} through S_j are

$$h_j = S_j^T \left((M_{B_j}^0 \dot{S}_j + \dot{M}_{B_j}^0 S_j) \dot{q}_j + \dot{M}_{B_j}^0 V_1^0 \right).$$

d) Gravitational terms: The gravitational wrench acting at the center of mass of body B_j is

$$W_{\text{grav}, B_j}^0 = M_{B_j}^0 G^0, \quad G^0 = \text{col}(0_5, -g_r),$$

where g_r is the gravitational acceleration. The base component g_b and B_j 's gravitational wrench projected onto the corresponding joint J_{1j} through S_j are respectively calculated by

$$g_b = - \sum_{j=1}^5 W_{\text{grav}, B_j}^0, \quad g_p = -S_p^T \text{col}(W_{\text{grav}, B_j}^0).$$

e) Applied external wrenches: The external wrench applied at the base B_1 's center of mass and expressed in the world frame is

$$W_{\text{app}, b}^0 = \sum_{j=2}^5 W_{\text{app}, B_j}^0 = \sum_{j=2}^5 \text{Ad}_{(C_{J_j}^0)^{-1}} \bar{f}_j$$

where $W_{\text{app}, B_j}^0 \in se(3)^*$ represents the applied spatial wrench at B_j 's CoM. The external wrenches acting on the pendulum links B_2, B_3, B_4 projected onto the joints are

$$W_{\text{app}, p}^0 = S_p^T \text{col}(W_{\text{app}, B_j}^0).$$

The total applied wrench vector is therefore

$$W_{\text{app}}^0 = (W_{\text{app}, b}^0 \quad W_{\text{app}, p}^0)^T.$$

B. Efficient Implementation of the Controller

We introduce here a novel version of the Articulated-body Inertia Algorithm (ABA), originally derived in [25], which is modified to recursively obtain the acceleration $(\ddot{q}_t, \dot{V}_1^0)$ needed to implement the feedback linearizing law (7) (9) efficiently, instead of inverting the mass matrix M in (1).

For the system in Fig. 1, a modified ABA computes $(\ddot{q}_t, \dot{V}_1^0)$ executing the following computations for each $j = 2, 3, 4$

$$\begin{aligned} M_{j2}^A &= M_{B_j}^0 \\ \psi_{j2} &= (S_{j2}^T M_{j2}^A S_{j2})^{-1} \\ W_{j2}^A &= -\text{ad}_{V_{j2}^0}^T M_{B_j}^0 V_{j2}^0 - W_{\text{app}, B_j}^0 - W_{\text{grav}, B_j}^0 \\ M_{j1}^A &= M_{j2}^A - M_{j2}^A S_{j2} \psi_{j2} S_{j2}^T M_{j2}^A \\ \psi_{j1} &= (S_{j1}^T M_{j1}^A S_{j1})^{-1} \\ W_{j1}^A &= M_{j2}^A \left(S_{j2} \ddot{q}_{j2} + \dot{S}_{j2} \dot{q}_{j2} \right) + W_{j2}^A \end{aligned}$$

where \ddot{q}_{ji} , with $i = 1, 2$, is given by:

$$\ddot{q}_{ji} = \psi_{ji} \left(\tau_{f_{ji}} - S_{ji}^T \left(M_{ji}^A \dot{S}_{ji} \dot{q}_{ji} + W_{ji}^A \right) \right)$$

Afterwards, the articulated inertia M_1^A and bias wrench W_1^A for the base are computed as

$$\begin{aligned} M_1^A &= M_{B_1}^0 + M_{B_5}^0 + \sum_{j=2}^4 (M_{j1}^A - M_{j1}^A S_{j1} \psi_{j1} S_{j1}^T M_{j1}^A), \\ W_1^A &= -\text{ad}_{V_1^0}^T (M_{B_1}^0 + M_{B_5}^0) V_1^0 - W_{app, B_1}^0 - W_{grav, B_1}^0 - W_{grav, B_5}^0 \\ &\quad + \sum_{j=2}^4 (M_{j1}^A (S_{j1} \ddot{q}_{j1} + \dot{S}_{j1} \dot{q}_{j1}) + W_{j1}^A). \end{aligned}$$

Hence, the following six linear equations are solved for the base acceleration twist \dot{V}_1^0 using LDL^T method, since M_1^A is symmetric positive definite

$$0 = M_1^A \dot{V}_1^0 + W_1^A.$$

The obtained value of \dot{V}_1^0 is then used to retrieve the joint accelerations by evaluating the following expressions:

$$\begin{aligned} \ddot{q}_{j1} &= -\psi_{j1} S_{j1}^T M_{j1}^A \dot{V}_1^0 + \ddot{q}_{j1} \\ \dot{V}_{j1}^0 &= \dot{V}_1^0 + S_{j1} \ddot{q}_{j1} + \dot{S}_{j1} \dot{q}_{j1} \\ \ddot{q}_{j2} &= -\psi_{j2} S_{j2}^T M_{j2}^A \dot{V}_{j1}^0 + \ddot{q}_{j2}. \end{aligned}$$

C. Lemma 1 and its proof

Lemma 1. Consider a vehicle with a thrust magnitudes vector $f = \text{col}(f_i) \in \mathbb{R}_{\geq 0}^l$ with the corresponding propellers configurations $C_i^0(C_1^0, \alpha_i) \in SE(3)$, relative to a right-handed inertial frame whose z-axis direction opposes the axis along which the gravitational force is applied, where $C_1^0 \in SE(3)$ is the base configuration and $\alpha_i \in \mathbb{S}^2$ is the unit direction vector of the propeller i expressed in the inertial frame. At any equilibrium for the MAV with a given C_1^0 , there is no internal force generated at such equilibrium if and only if all propellers, whose thrust magnitudes are $f_i > 0$, are pointing in the direction of inertial frame's z-axis, i.e. $C_i^0(C_1^0, \alpha_i) e_3 = e_3 \forall i \in \{1, \dots, l\}$ with $e_3 = (0010)^T$.

1) *Necessity Proof:* Assume that at least one propeller, labeled l , is not vertical in the inertial frame, hence $C_l^0(C_1^0, \alpha_l) e_3 \neq e_3$. The thrust force vector of propeller i , expressed in the inertial frame, is denoted by $T_i^0 = f_i \alpha_i$. When the MAV is at equilibrium, the resultant thrust force in the inertial frame must satisfy $T_{tot}^0 = m_{tot} g_r (001)^T$ to compensate for the gravitational force. Thus, this constraint must hold at equilibrium

$$\begin{aligned} \sum_{i=1}^{l-1} f_i (001)^T + f_l (\alpha_{lx} \ \alpha_{ly} \ \alpha_{lz})^T &= m_{tot} g_r (001)^T (10) \\ \sqrt{\alpha_{lx}^2 + \alpha_{ly}^2 + \alpha_{lz}^2} &= 1 \end{aligned} \quad (11)$$

Expanding this yields

$$f_l \alpha_{lx} = 0, \quad f_l \alpha_{ly} = 0, \quad f_l \alpha_{lz} = m_{tot} g_r - \sum_{i=1}^{l-1} f_i \quad (12)$$

If $f_l > 0$ then (12) gives $(\alpha_{lx}, \alpha_{ly}) = (0, 0)$. This makes (11) have only two possible solution $\alpha_{lz} = \pm 1$. Setting $\alpha_{lz} = 1$ in (12) yields $\sum_{i=1}^{l-1} f_i < m_{tot} g_r$. This

solution for α_l is in a contradiction with the assumption as it implies that $C_l^0(C_1^0, \alpha_l) e_3 = e_3$ is true, i.e. propeller l is vertical in the inertial frame, and (12) admits a solution of $f_i = \frac{1}{l} m_{tot} g_r$. As a result, $f \in \mathcal{F}_{min}^{eq}$ and no internal force is generated at equilibrium. If instead $f_l > 0$ and $(\alpha_{lx}, \alpha_{ly}, \alpha_{lz}) = (0, 0, -1)$, then from (12) we have $\sum_{i=1}^{l-1} f_i > m_{tot} g_r$. While this is not a contradiction, it leads to $f \in \mathcal{F}_{int.for.}^{eq}$. Hence, the assumption $C_l^0(C_1^0, \alpha_l) e_3 \neq e_3$ does not hold when $f \in \mathcal{F}_{min}^{eq}$, proving the necessary condition by contradiction. By induction, the same steps can be easily repeated to cases where two or more propellers assume $C_l^0(C_1^0, \alpha_l) e_3 \neq e_3$.

2) *Sufficiency Proof:* If all propellers point up at equilibrium, i.e. $C_i^0(C_1^0, \alpha_i) e_3 = e_3 \forall i \in \{1, \dots, l\}$, then this renders all direction vectors α_i 's equal to $(001)^T$, which automatically satisfies (10) with $f_i = \frac{1}{l} m_{tot} g_r$. Hence, $f \in \mathcal{F}_{min}^{eq}$.

D. Proof of Proposition 1

The proof is constructive and divided into two parts. In the first part, Statement 1 is proven by finding PJD_2 joint equilibrium configurations $q_{pe}^{[2]}$ from (3) for any given base pose $C_{1e}^0 \in SE(3)$ and showing that the associated equilibrium thrust $f_e^{[2]}$ belongs to the minimal equilibrium thrust \mathcal{F}_{min}^{eq} defined in (4) and remains fixed for any such pose C_{1e}^0 , rendering Statement 2 an immediate corollary as the condition $f_e^{[2]} \in \mathcal{F}_{min}^{eq}$ implies that no excess thrust is present at any C_{1e}^0 , i.e. $f_e^{[2]} \notin \mathcal{F}_{int.for.}^{eq}$. (Definition 1 (4)).

In the second part, we start by solving (2) for $q_{pe}^{[1]}$. We then illustrate that, when $\tau_{dj} \neq 0$, there is no joint equilibrium satisfying $C_j^0(C_{1e}^0, q_{je}^{[1]}) e_3 = e_3$, hence by Lemma 1, no minimal thrust is produced at these equilibria $q_{pe}^{[1]}$, which is the subject of statement 3. Once again, statement 4 follows as a result since $C_j^0(C_{1e}^0, q_{je}^{[1]}) e_3 \neq e_3$ necessarily implies $f_e^{[1]} \in \mathcal{F}_{int.for.}^{eq}$. However, we observe that $f_e^{[1]}$, when $\tau_{dj} \neq 0$, $f_e^{[1]}$ can be made arbitrarily close to the set \mathcal{F}_{min}^{eq} (4), i.e. $q_{pe}^{[1]}$ is arbitrarily close to meet $C_j^0(C_{1e}^0, q_{je}^{[1]}) e_3 = e_3$, by changing the link parameters. Lastly, we give the definitions of the equilibria sets for the state and thrust.

1) *Statement 1 Proof:* Expanding the LHS of (3) or (2) for any $B_j \forall j = 2, 3, 4$ yields the pair of equations for B_j

$$g_{pj} = -S_j^T W_{grav, B_j}^0 = (-S_{j1}^T \quad -S_{j2}^T)^T M_{B_j}^0 G^0 \quad (13)$$

where the instantaneous spatial screws are given by $S_{j1}(C_1^0) = \text{Ad}_{C_1^0} Y_{j1}$ and $S_{j2}(C_1^0, q_{j1}) = \text{Ad}_{C_{j1}^0} \text{Ad}_{A_{j1}^0}^{-1} Y_{j2}$, with A_{j1}^0 being the configuration of the intermediate link \bar{B}_j frame, placed at the center of rotation of q_{j1} , connecting B_1 and B_j when the vehicle is in the home configuration shown in Fig. 1, and C_{j1}^0 being its configuration in a generic vehicle pose. $Y_{ji} \in \mathbb{R}^6$ is the constant spatial screw of q_{ji} in home configuration. For details on screw theory, consult [26].

Now, consider the LHS of first equation in (13), which is written as

$$\begin{aligned} g_{pj1} &= -S_{j1}^T M_{B_j}^0 (0_{1 \times 5} \quad -g_r)^T \\ &= Y_{j1}^T \text{Ad}_{C_1^0}^T \text{Ad}_{C_j^0}^{-T} I_{B_j}^T \text{Ad}_{C_j^0}^{-1} e_6^6 g_r \end{aligned} \quad (14)$$

where $I_{B_j}^j$ is the diagonal B_j 's CoM-referred inertia tensor. $\bar{e}_i^k \in \mathbb{R}^k$ is a zero vector with 1 in the i -th component. Since the adjoint matrix $\text{Ad}_{C_j^0}^{-T}$ has the properties

$$\begin{aligned} \text{Ad}_{C_j^0}^{-T} &= \text{Ad}_{C_j^0}^T = (\text{Ad}_{C_1^j C_0^1})^T = (\text{Ad}_{C_1^j} \text{Ad}_{C_0^1})^T \\ &= \text{Ad}_{C_0^1}^T \text{Ad}_{C_1^j}^T = \text{Ad}_{C_0^1}^{-T} \text{Ad}_{C_1^j}^{-T} \end{aligned} \quad (15)$$

substituting $\text{Ad}_{C_j^0}^{-T} = \text{Ad}_{C_0^1}^{-T} \text{Ad}_{C_1^j}^{-T}$ in (14) gives

$$g_{p_{j1}} = Y_{j1}^T \text{Ad}_{C_1^j}^{-T} I_{B_j}^j \text{Ad}_{C_0^1}^{-1} \bar{e}_6^6 g_r = Y_{j1}^T \text{Ad}_{C_1^j}^{-T} I_{B_j}^j \bar{r}_j g_r \quad (16)$$

where \bar{r}_j denotes

$$\bar{r}_j = \text{Ad}_{C_0^1}^{-1} \bar{e}_6^6 \quad (17)$$

Observe that substituting $\bar{r}_j = \bar{e}_6^6$ in (16) reduces it to

$$\begin{aligned} g_{p_{j1}} &= Y_{j1}^T \text{Ad}_{C_1^j}^{-T} I_{B_j}^j \bar{e}_6^6 g_r \\ &= Y_{j1}^T \text{Ad}_{C_1^j}^{-T} \bar{e}_6^6 m_p g_r \end{aligned} \quad (18)$$

where $g_{p_{j1}}$ now depends only on q_j . Since the constant screw is $Y_{j1}^T = ((\bar{e}_1^3)^T \sigma_j \frac{a}{2} (\bar{e}_3^3)^T)^T$, where $\sigma_j = 1$ for $j = 2, 5$ and $\sigma_j = -1$ otherwise, (18) can be manipulated further as

$$\begin{aligned} g_{p_{j1}} &= ((\bar{e}_1^3)^T \sigma_j \frac{a}{2} (\bar{e}_3^3)^T) \begin{pmatrix} R_j^1 & -(P_j^1)^T \times R_j^1 \\ 0_{3 \times 3} & R_j^1 \end{pmatrix} \bar{e}_6^6 m_p g_r \\ &= ((\bar{e}_1^3)^T \sigma_j \frac{a}{2} (\bar{e}_3^3)^T) \begin{pmatrix} -(P_j^1)^T \times R_j^1 \bar{e}_3^3 \\ R_j^1 \bar{e}_3^3 \end{pmatrix} m_p g_r \\ &= (\sigma_j \frac{a}{2} (\bar{e}_3^3)^T - (\bar{e}_1^3)^T (P_j^1)^T) R_j^1 \bar{e}_3^3 m_p g_r \\ &= 0 \equiv \text{RHS of first equation in (3)}. \end{aligned}$$

where $C_j^1 = \begin{pmatrix} R_j^1 & P_j^1 \\ 0_{1 \times 3} & 1 \end{pmatrix}$. Hence setting $\bar{r}_j = \bar{e}_6^6$ satisfies the first equation in (3).

Next, let us consider the second equation in (3). Simplifying using the properties in (15), and substituting the expression of the constant screw Y_{j2} , configuration A_{j1}^0 and \bar{r}_j (17) yield

$$\begin{aligned} g_{p_{j2}} &= Y_{j2}^T \text{Ad}_{A_{j1}^0}^{-T} \text{Ad}_{C_{j1}^0}^T \text{Ad}_{C_j^0}^{-T} I_{B_j}^j \text{Ad}_{C_j^0}^{-1} \bar{e}_6^6 g_r \\ &= Y_{j2}^T \text{Ad}_{A_{j1}^0}^{-T} \text{Ad}_{C_{j1}^0}^{-T} I_{B_j}^j \bar{r}_j g_r \\ &= ((\bar{e}_2^3)^T 0_{1 \times 3}) \text{Ad}_{C_{j1}^0}^{-T} I_{B_j}^j \bar{r}_j g_r \end{aligned} \quad (19)$$

Setting $\bar{r}_j = \bar{e}_6^6$ gives

$$\begin{aligned} g_{p_{j2}} &= ((\bar{e}_2^3)^T 0_{1 \times 3}) \text{Ad}_{C_{j1}^0}^{-T} \bar{e}_6^6 m_p g_r \\ &= ((\bar{e}_2^3)^T 0_{1 \times 3}) \begin{pmatrix} -(P_j^1)^T \times R_j^1 \bar{e}_3^3 \\ R_j^1 \bar{e}_3^3 \end{pmatrix} m_p g_r \\ &= -(\bar{e}_2^3)^T (P_j^1)^T \times R_j^1 \bar{e}_3^3 m_p g_r \\ &= \begin{pmatrix} -\cos(q_{j2e}) & 0 & \sin(q_{j2e}) \\ 0 & \cos(q_{j2e}) & 0 \end{pmatrix} \begin{pmatrix} \sin(q_{j2e}) \\ 0 \\ \cos(q_{j2e}) \end{pmatrix} c m_p g_r \\ &= 0 \equiv \text{RHS of second equation in (3)}. \end{aligned}$$

We conclude that $\bar{r}_j = \bar{e}_6^6$ satisfies (3). Observe that this condition implies that all propellers are aligned vertically in

the inertial frame at equilibria for any $C_{1e}^0 \in SE(3)$. To see this, expand (17) as

$$\begin{aligned} \bar{r}_j &= \bar{e}_6^6 = \text{Ad}_{C_j^0}^{-1} \bar{e}_6^6 \\ \begin{pmatrix} 0_{3 \times 1} \\ \bar{e}_3^3 \end{pmatrix} &= \begin{pmatrix} R_0^j & 0_{3 \times 3} \\ -R_0^j (P_j^0) \times & R_0^j \end{pmatrix} \begin{pmatrix} 0_{3 \times 1} \\ \bar{e}_3^3 \end{pmatrix} = \begin{pmatrix} 0_{3 \times 1} \\ R_0^j \bar{e}_3^3 \end{pmatrix} \end{aligned}$$

Hence $\bar{e}_3^3 = R_0^j (R_{1e}^0, q_{je}^{[2]}) \bar{e}_3^3 \forall j = 2, 3, 4, 5$, or alternatively $C_j^0 e_3 = e_3$ using Lemma 1 notation. This also gives the expression of $q_{je}^{[2]}$ by solving $\bar{r}_j = \bar{e}_6^6$ for $q_{je}^{[2]}$ as

$$R_0^1 e \bar{e}_3^3 = R_j^1 (q_{je}^{[2]}) \bar{e}_3^3 = R_x (q_{j1e}^{[2]}) R_y (q_{j2e}^{[2]}) \bar{e}_3^3$$

Thus we have the solution $q_{je}^{[2]}$ as

$$\begin{aligned} l_{s1} &= \frac{-r_{32}}{\sqrt{1-r_{31}^2}}, l_{c1} = \sqrt{1-l_{s1}^2} \\ l_{s2} &= r_{31}, l_{c2} = \sqrt{1-l_{s2}^2} \\ q_{jie}^{[2]} &= \text{atan}(l_{si}, l_{ci}) \forall i = 1, 2, j = 2, 3, 4, 5 \end{aligned} \quad (20)$$

where r_{mn} is the element (m, n) in any desired base orientation at PJD₂ equilibrium R_{1e}^0 . Notice that $q_{je}^{[2]}$ is equal for any attached link B_j . Moreover, it is always possible to obtain this solution $q_{je}^{[2]}$ (20) for every $R_0^1 \in SO(3)$ since aligning the unit vector $R_j^1 (q_{je}^{[2]}) \bar{e}_3^3 =: z_j^1$, where $z_j^1 \in \mathbb{S}^2$ is the z-axis of \mathcal{F}_{p_j} expressed in \mathcal{F}_b , with any desired unit vector $z_0^1 \in \mathbb{S}^2$ in \mathcal{F}_b , where $R_0^1 \bar{e}_3^3 =: z_0^1$, requires only 2 variables, i.e. $q_{j1e}^{[2]}, q_{j2e}^{[2]}$, as $\dim(\mathbb{S}^2) = 2$ when the manifold \mathbb{S}^2 is embedded in the 3-dimensional Euclidean vector space.

Now, we show that the associated thrust $f_e^{[2]} \in \mathcal{F}_{\min}^{\text{eq}}$ and fixed for any C_{1e}^0 . The dynamics of base at any static equilibrium reduces to

$$g_b(C_{1e}^0, q_{pe}) = -W_{\text{app}, b}^0(f_e, q_{pe}, q_{ae})$$

which reads explicitly as

$$\sum_{j=2}^5 \text{Ad}_{(C_{j1}^0)^{-1}}^T \bar{f}_j f_{je} = \sum_{j=1}^5 \text{Ad}_{(C_j^0)^{-T}} I_{B_j}^j \text{Ad}_{(C_j^0)^{-1}} \bar{e}_6^6 g_r$$

Substituting $\bar{r}_j = (0_{3 \times 1} \ r_{gj})$ from (17) yields

$$\begin{aligned} \sum_{j=2}^5 \left((Ik_j - (P_j^1)^T \times R_j^1 \bar{e}_3^3) f_{je} = g_r m_b \begin{pmatrix} 0_{3 \times 1} \\ R_0^1 \bar{e}_3^3 \end{pmatrix} \right. \\ \left. + g_r \sum_{j=2}^5 m_j \begin{pmatrix} -(P_j^1)^T \times R_j^1 r_{gj} \\ R_j^1 r_{gj} \end{pmatrix} \right) \end{aligned}$$

where I is the identity matrix. Using the property $R_j^1 (R_1^j P_j^1) \times = -(P_j^1)^T \times R_j^1$ and $R_j^1 r_{gj} = R_0^1 \bar{e}_3^3$, we get

$$\begin{aligned} \sum_{j=2}^5 R_j^1 (Ik_j + (R_1^j P_j^1) \times) \bar{e}_3^3 f_{je} &= g_r \left(\sum_{j=2}^5 R_j^1 (R_1^j P_j^1) \times r_{gj} m_j \right) \\ \sum_{j=2}^5 R_j^1 \bar{e}_3^3 f_{je} &= g_r \sum_{j=2}^5 R_j^1 r_{gj} \left(\frac{1}{4} m_b + m_j \right) \end{aligned} \quad (21)$$

Since in PJD₂, $q_{je}^{[2]} \forall j = 2, 3, 4, 5$ are equal, R_j^1 can be taken as a common factor, hence pre-multiplying by R_j^1 gives

$$\sum_{j=2}^5 k_j f_{je}^{[2]} \bar{e}_3^3 + \sum_{j=2}^5 (R_1^j P_j^1)_{\times} f_{je}^{[2]} \bar{e}_3^3 = g_r \left(\sum_{j=2}^5 (R_1^j P_j^1)_{\times} m_j \right) \bar{e}_3^3$$

$$\bar{e}_3^3 \sum_{j=2}^5 f_{je}^{[2]} = \bar{e}_3^3 \sum_{j=2}^5 g_r \left(\frac{1}{4} m_b + m_j \right)$$

After $r_{g_j} = \bar{e}_3^3$ is substituted. The second equation is satisfied with $f_{je}^{[2]} = g_r (\frac{1}{4} m_b + m_j)$, hence $f_e^{[2]} \in \mathcal{F}_{\min}^{\text{eq}}$. Substituting this $f_{je}^{[2]}$ make the first equation reduce to

$$\sum_{j=2}^5 k_j g_r \left(\frac{1}{4} m_b + m_j \right) \bar{e}_3^3 + \sum_{j=2}^5 (R_1^j P_j^1)_{\times} \bar{e}_3^3 = 0$$

thus $\sum_{j=2}^5 k_j (\frac{1}{4} m_b + m_j) = 0$ since $\sum_{j=2}^5 (R_1^j P_j^1)_{\times} \bar{e}_3^3 = 0$ is always true at any $q_{je}^{[2]}$ (20). We conclude that the associated thrust at $q_{je}^{[2]}$ is, when $m_j = m_p \forall j = 2, 3, 4, 5$

$$f_{je}^{[2]} = g_r \left(\frac{1}{4} m_b + m_p \right), \text{ with } k_i \text{ chosen by } \sum_{j=2}^5 k_i = 0 \quad (22)$$

2) *Statement 2 Proof:* Since $f_e^{[2]} \in \mathcal{F}_{\min}^{\text{eq}}$ is proven in Statement 1, it follows from Definition 1 that no internal forces are generated $f_e^{[2]} \notin \mathcal{F}_{\text{int.for.}}^{\text{eq}}$ at the corresponding equilibrium configurations associated with this $f_e^{[2]}$, i.e. $q_{te}^{[2]}$ in (20) and any desired $C_{1e}^0 \in SE(3)$.

3) *Statement 3 Proof:* In Sec. D.1, it is found that when all propellers point up in the inertial frame, i.e. $\bar{r}_j = \bar{e}_6^0$ or $C_j^0 e_3 = e_3 \forall j = 2, 3, 4, 5$, the LHS of (2) becomes $g_{p_j}(C_{1e}^0, q_{pe}) = 0$. Since the RHS of it for any j is equal to (τ_{dj}^0) , which is not zero when $\tau_{dj} \neq 0$, $C_j^0(C_{1e}^0, q_{je}^{[1]}) e_3 \neq e_3$ must hold true. Thus, from Lemma 1, no minimal thrust is produced at any PJD₁ equilibrium $f_e^{[1]} \notin \mathcal{F}_{\min}^{\text{eq}} \forall \tau_{dj} \neq 0$.

For completeness, we proceed to find conditions on $q_{pe}^{[1]}$, similar to $\bar{r}_j = \bar{e}_6^0$ obtained for PJD₂, that must be met at any base equilibrium C_{1e}^0 . We start from (19) and substitute the values of the constant screws, constant transformations and $\bar{r}_j = (0_{3 \times 1} \ r_{g_j})$, which yields

$$-(\bar{e}_2^3)^T (P_j^{j1})_{\times}^T R_j^{j1} r_{g_j} m_j g_r = 0$$

which is satisfied when $r_{g_j} = (0 \ r_{g_{j,1}} \ r_{g_{j,2}})$, $r_{g_{j,2}} = \sqrt{1 - r_{g_{j,1}}^2}$. In PJD₁, (16) has the RHS equal to $S_{j1}^T W_{app,B_j}^0$. This can be expressed as

$$\left(\sigma_j \frac{a}{2} (\bar{e}_3^3)^T - (\bar{e}_1^3)^T (P_j^1)_{\times}^T R_j^1 (r_{g_j} m_j g_r - \bar{e}_3^3 f_{je}^{[1]}) \right. \\ \left. + (\bar{e}_1^3)^T R_j^1 \bar{e}_3^3 k_j f_{je}^{[1]} = 0 \right)$$

since

$$Y_{j1}^T \text{Ad}_{C_j^1}^{-T} = (\cos(q_{j2e}) \ 0 \ \sin(q_{j2e}) \ 0 \ c \ \cos(q_{j2e}) \ 0)$$

hence $q_{j2e}^{[1]}$ is constraint by

$$\cos(q_{j2e}^{[1]}) = \pm \sqrt{\frac{k_j^2 (f_{je}^{[1]})^2}{c^2 m_j^2 g_r^2 r_{g_{j,1}}^2 + k_j^2 (f_{je}^{[1]})^2}}$$

Lastly, from (21), we have these conditions on $R_j^1(q_{je}^{[1]})$, $f_{je}^{[1]}$

$$\sum_{j=2}^5 R_j^1 k_j \bar{e}_3^3 f_{je}^{[1]} = 0, \quad R_j^1 r_{g_j} = R_0^1 \bar{e}_3^3$$

$$\sum_{j=2}^5 (P_j^1)_{\times} (R_j^1 \bar{e}_3^3 f_{je}^{[1]} - R_j^1 r_{g_j} g_r m_j) = 0 \quad (23)$$

$$\sum_{j=2}^5 R_j^1 \bar{e}_3^3 f_{je}^{[1]} - \sum_{j=2}^5 R_j^1 r_{g_j} g_r \left(\frac{1}{4} m_b + m_j \right) = 0$$

4) *Statement 4 Proof:* By definition 1, and Statement 3, $f_e^{[1]} \in \mathcal{F}_{\text{int.for.}}^{\text{eq}}$ immediately follows as a corollary. The amount of internal force can be made arbitrarily small if solutions of (3) and (2) are made arbitrarily close, which is realized by making the term $\frac{k_j}{cm_j} = 0$, i.e. reducing the drag-to-thrust coefficient or increasing the pendulum length or mass.

Finally, we conclude the proposition proof by defining the equilibria state sets as

$$\mathbb{D}_{x_e}^{[i]} = \left\{ x(t) \in \mathbb{X}, \{t, \bar{t}\} \in \mathbb{R}_{\geq 0} \mid \forall C_{1e}^0 \in SE(3), \forall t \geq \bar{t}, \right. \\ \left. x(t) := (C_1^0(t), q_p(t), V_1^0, \dot{q}_p, q_a(t))^T \right. \\ \left. = (C_{1e}^0(\bar{t}), q_{pe}^{[i]}(\bar{t}), 0_{12}, q_{ae}^{[i]}(\bar{t})) \right\} \\ q_{pe}^{[i]} \text{ from (23) or (20), for } i = 1, 2, \text{ respectively} \Big\}$$

while the associated thrust equilibrium sets are given by

$$\mathbb{D}_{f_e}^{[i]} = \left\{ f(t) \in \mathbb{R}^4, \{t, \bar{t}\} \in \mathbb{R}_{\geq 0} \mid \forall t \geq \bar{t}, f(t) = f_e^{[i]}(\bar{t}), \right. \\ \left. f_e^{[i]} \text{ from (23) or (22), for } i = 1, 2, \text{ respectively} \right\}$$

E. Proof of Theorem 1

The proof relies on the relative degree notion for MIMO affine nonlinear systems [27] and the dynamic extension algorithm for invertible systems [24] to prove Statement 1. Afterwards, we show that Statement 2 is true by a standard Lyapunov argument applied to the zero dynamics in the normal form.

1) *Statement 1 Proof:* To compute the relative degree of Σ_2 w.r.t. V_1^0 , we take time derivatives of the output V_1^0

$$\dot{h}_y = \dot{V}_1^0$$

From (1) \dot{V}_1^0 is expressed as

$$M_{bb} \dot{V}_1^0 = -M_{bp} \ddot{q}_p - h_b - g_b + W_{app,b}^0 \quad (24)$$

Following the approach of [28] we can express \ddot{q}_p in terms of \dot{V}_1^0 , $W_{app,p}^0$ and τ_f , hence

$$\ddot{q}_p = L_1 - M_{pp}^{-1} M_{bp}^T \dot{V}_1^0 + M_{pp}^{-1} W_{app,p}^0$$

where L_1 is defined as

$$L_1 := M_{pp}^{-1} (\tau_f - h_t - g_p) \quad (25)$$

Substituting in (24) gives

$$(M_{bb} - M_{bp}M_{pp}^{-1}M_{bp}^T)\dot{V}_1^0 = -M_{bp}L_1 - h_b - g_b + W_{app,b}^0 - M_{bp}M_{pp}^{-1}W_{app,p}^0$$

which can be compactly rewritten as

$$\dot{h}_y = \dot{V}_1^0 = E_1 + M_b^{-1}D_1u \quad (26)$$

where M_b , D_1 and E_1 are defined as, with $j = 2, 3, 4$

$$\begin{aligned} M_b &= (M_{bb} - M_{bp}M_{pp}^{-1}M_{bp}^T) \\ N_j &= (I_6 - M_{B_j}^0 S_j (S_j^T M_{B_j}^0 S_j)^{-1} S_j^T) \\ \bar{D}_1 &= \begin{pmatrix} N_j \text{Ad}_{(C_{f_j}^0)^{-1}} \bar{f}_j & \cdots & \text{Ad}_{(C_{f_5}^0)^{-1}} \bar{f}_5 \end{pmatrix} \\ D_1 &= \begin{pmatrix} \bar{D}_1 & 0_{6 \times 2} \end{pmatrix} \\ E_1 &= M_b^{-1}(-M_{bp}L_1 - h_b - g_b) \end{aligned} \quad (27)$$

Note that $(S_j^T M_{B_j}^0 S_j) \in R^{2 \times 2}$ is a symmetric positive definite matrix.

Since the decoupling matrix $M_b^{-1}D_1$ is singular due to D_1 being singular of rank 4 $\forall x_e \in \mathbb{D}_{x_e}^{[2]}$, system (5) does not have a vector relative degree in any open neighbourhood of the equilibrium $x_e \in \mathbb{D}_{x_e}^{[2]}$. Thus, the system is not I/O feedback linearizable by any static state feedback as the relative degree is invariant under this kind of feedback [27].

However, extending the system dynamics Σ_2 with an input precompensator, by applying the version of the dynamic extension algorithm presented in [24] for invertible nonlinear systems, results in a system for which the vector relative degree is well-defined. Assume the precompensator takes this pure integrator form (6). Let $\bar{x} \in \bar{\mathbb{X}}$ be the extended state and $w \in \mathbb{R}^6$ the new input. The extended system $\Sigma_{\bar{2}}$ can be written as $\Sigma_{\bar{2}}: \dot{\bar{x}} = \bar{F}_2 + \bar{G}_2 w$ with $\bar{F} := F_2 + G_2 \bar{u}$, where $\bar{u} = (z, 0, 0)^T$ and \bar{G}_2 is given by

$$\bar{G}_2 = \begin{pmatrix} 0_{18 \times 6} \\ 0_{2 \times 4} & I_{2 \times 2} \\ I_{4 \times 4} & 0_{2 \times 2} \end{pmatrix}$$

Now, we can proceed with computing the vector relative degree of $\Sigma_{\bar{2}}$ w.r.t V_1^0 by differentiating \dot{h}_y w.r.t time

$$M_{bb}\ddot{V}_1^0 = -\dot{M}_{bp}\ddot{q}_p - M_{bp}\ddot{q}_p + \dot{W}_{app,b}^0 - \dot{M}_{bb}\dot{V}_1^0 - \dot{h}_b - \dot{g}_b$$

by substituting this expression for \ddot{q}_p

$$\ddot{q}_p = L_2 - M_{pp}^{-1}M_{bp}^T \dot{V}_1^0 + M_{pp}^{-1}\dot{W}_{app,p}^0$$

where L_2 is defined as

$$L_2 := M_{pp}^{-1}((\dot{\tau}_f - \dot{h}_p - \dot{g}_p) - (\dot{M}_{bp}^T \dot{V}_1^0 + \dot{M}_{pp}\ddot{q}_p)) \quad (28)$$

and after some algebraic manipulation it yields

$$\begin{aligned} M_b\ddot{V}_1^0 &= -\dot{M}_{bp}(L_1 + M_{pp}^{-1}W_{app,p}^0) - M_{bp}L_2 \\ &+ (\dot{M}_{bp}M_{pp}^{-1}M_{bp}^T - \dot{M}_{bb})\dot{V}_1^0 - \dot{h}_b - \dot{g}_b \\ &- M_{bp}M_{pp}^{-1}\dot{W}_{app,p}^0 + \dot{W}_{app,b}^0 \end{aligned} \quad (29)$$

where the $\dot{h}_b, \dot{g}_b, \dot{h}_p, \dot{g}_p, \dot{M}, \dot{S}_j, \dot{W}_{app,B_j}^0$ are given by

$$\begin{aligned} \dot{h}_b &= \sum_{j=2}^4 ((M_{B_j}^0 \dot{S}_j + \dot{M}_{B_j}^0 S_j + 2\dot{M}_{B_j}^0 \dot{S}_j)\dot{q}_j \\ &+ (M_{B_j}^0 \dot{S}_j + \dot{M}_{B_j}^0 S_j)\ddot{q}_j) + \dot{M}_{bb}V_1^0 + \dot{M}_{bb}\dot{V}_1^0 \\ \dot{h}_p &= \text{col}(\dot{S}_j^T ((M_{B_j}^0 \dot{S}_j + \dot{M}_{B_j}^0 S_j)\dot{q}_j + \dot{M}_{B_j}^0 V_1^0) \\ &+ S_j^T ((M_{B_j}^0 \dot{S}_j + \dot{M}_{B_j}^0 S_j + 2\dot{M}_{B_j}^0 \dot{S}_j)\dot{q}_j \\ &+ (M_{B_j}^0 \dot{S}_j + \dot{M}_{B_j}^0 S_j)\ddot{q}_j + \dot{M}_{B_j}^0 V_1^0 + \dot{M}_{B_j}^0 \dot{V}_1^0)) \\ \dot{g}_b &= -(\dot{M}_{bb} + \dot{M}_{B_5}^0)G^0 \\ \dot{g}_p &= -\dot{S}_p^T \text{col}(M_{B_j}^0 G^0) - S_p^T \text{col}(\dot{M}_{B_j}^0 G^0) \\ \dot{M}_{B_j}^0 &= M_{B_j}^0 \text{ad}_{V_k^0}^2 + (\text{ad}_{V_k^0}^2)^T M_{B_j}^0 + 2 \text{ad}_{V_k^0}^T M_{B_j}^0 \text{ad}_{V_k^0} \\ &- M_{B_j}^0 \text{ad}_{V_k^0} - \text{ad}_{V_k^0}^T M_{B_j}^0, \text{ if } k=5 \text{ then } V_k^0 = V_1^0, \dot{V}_k^0 = \dot{V}_1^0 \\ \dot{S}_k &= (\text{ad}_{V_k^0} + \text{ad}_{V_k^0}^2)S_k, k=2,3,4 \\ \dot{W}_{app,B_k}^0 &= -\text{ad}_{V_k^0}^T W_{app,B_k}^0 + \text{Ad}_{(C_{f_5}^0)^{-1}} \dot{W}_{app,B_k}^0, k=2,3,4,5 \end{aligned} \quad (30)$$

where $j = 2, 3, 4$. Note that $M_{B_5}^0$ depends only on C_1^0 , i.e. $M_{B_5}^0(C_1^0)$, due to the assumptions on link B_5 . Hence, the input \dot{q}_a does not appear in $\dot{M}_{B_5}^0(C_1^0)$. Observe that (29) can be compactly put in the form,

$$\ddot{h}_y = \ddot{V}_1^0 = E_2 + M_b^{-1}D_2w$$

where E_2 and D_2 are calculated from, with $j = 2, 3, 4$

$$\begin{aligned} D_2 &= \begin{pmatrix} N_j \text{Ad}_{(C_{f_j}^0)^{-1}} \bar{f}_j & \cdots & \text{Ad}_{(C_{f_5}^0)^{-1}} \bar{f}_5 & \bar{D}_2 \end{pmatrix} \\ \bar{D}_2 &= \begin{pmatrix} -\text{ad}_{S_{51}}^T \text{Ad}_{(C_{f_5}^0)^{-1}} \bar{f}_5 z_5 & -\text{ad}_{S_{52}}^T \text{Ad}_{(C_{f_5}^0)^{-1}} \bar{f}_5 z_5 \end{pmatrix} \\ E_2 &= M_b^{-1}(-\dot{M}_{bp}(L_1 + M_{pp}^{-1}W_{app,p}^0) - M_{bp}L_2 \\ &+ (\dot{M}_{bp}M_{pp}^{-1}M_{bp}^T - \dot{M}_{bb})\dot{V}_1^0 - \dot{h}_b - \dot{g}_b + \bar{W}) \\ \bar{W} &= -\sum_{j=2}^4 B_j \text{ad}_{V_{j2}^0}^T W_{app,B_j}^0 - \text{ad}_{V_1^0}^T W_{app,B_5}^0 \end{aligned} \quad (31)$$

where L_1, L_2, M_b and N_j are given in (25), (28) and (27).

Because of the decoupling matrix $M_b^{-1}D_2$ of the extended system $\Sigma_{\bar{2}}$ being full rank equal to 6 in the open neighbourhood $\mathbb{U}_{\bar{x}_e} \subseteq \bar{\mathbb{X}}$ of equilibrium $\bar{x}_e \in \mathbb{D}_{x_e}^{[2]} \cup \mathbb{D}_{f_e}^{[2]}$, system $\Sigma_{\bar{2}}$ has a vector relative degree $(2, 2, 2, 2, 2, 2)$. Hence it can be transformed to a normal form $\Sigma_{\bar{2}}^H$ where the input/output map is linear by the means of the regular static state feedback w in (7) and the local diffeomorphism $H(\bar{x}) : \mathbb{U}_{\bar{x}_e} \rightarrow \mathbb{U}_{\bar{x}_e}$

$$\begin{pmatrix} \zeta_1 \\ \zeta_2 \\ \eta \end{pmatrix} = H(\bar{x}) := \begin{pmatrix} V_1^0 \\ E_1 + M_b^{-1}D_1u \\ \Phi(\bar{x}) \end{pmatrix} \quad (32)$$

where $\Phi(\bar{x}) : \mathbb{U}_{\bar{x}_e} \rightarrow \mathbb{T}^6 \times \mathbb{R}^6$ is a sufficiently smooth function chosen such that, in the open neighbourhood $\mathbb{U}_{\bar{x}_e}$, $H(\bar{x})$ is a diffeomorphism and $\frac{\partial \Phi}{\partial \bar{x}} \bar{G}_2 = 0$ holds. A possible choice of Φ is the states of the passive joints, as suggested in [28], $\Phi := (\eta_1, \eta_2)^T = (q_p, \dot{q}_p)^T$.

Hence the internal dynamics can be expressed as

$$\begin{aligned} \dot{\eta}_1 &= \eta_2 \\ \dot{\eta}_2 &= F_\eta(\eta_1, \eta_2, \zeta_1, \zeta_2, \bar{z}, C_1^0) \\ &:= L_1 - M_{pp}^{-1}M_{bp}^T \zeta_2 + M_{pp}^{-1}D_3 \bar{z} \end{aligned} \quad (33)$$

where η -dynamics represent the internal dynamics and D_3 ,

\bar{z} are calculated from

$$\bar{z} = \begin{pmatrix} z_2 & z_3 & z_4 \end{pmatrix}^T$$

$$D_3 = \text{blkdiag} \left((k_2 s_{22}, 0)^T, (k_3 s_{32}, 0)^T, (k_4 s_{42}, 0)^T \right) \quad (34)$$

where s_{jj} and c_{jj} are $\sin(q_{jj})$ and $\cos(q_{jj})$, respectively. Furthermore, we can map the controller states to the new coordinates $(z, q_a)^T = f_c(\zeta, \eta, C_1^0)$ where f_c is a solution of the algebraic equations

$$Q = \tilde{D}\bar{z} + L_3 z_5$$

where \tilde{D}, Q, L_3 are given by

$$\tilde{D} = \text{Ad}_{C_1^0}^T \begin{pmatrix} N_2 \text{Ad}_{(C_{f_2}^0)^{-1}} \bar{f}_2 & N_3 \text{Ad}_{(C_{f_3}^0)^{-1}} \bar{f}_3 & N_4 \text{Ad}_{(C_{f_4}^0)^{-1}} \bar{f}_4 \end{pmatrix}$$

$$Q = \text{Ad}_{C_1^0}^T M_b (\zeta_2 - E_1)$$

$$L_3 = \begin{pmatrix} \frac{k_5 s_{52} - \frac{a c_{51} c_{52}}{2}}{c_{52} (a c_{51} - 2 k_5 s_{51})} \\ \frac{a (s_{52} + c_{52} s_{51})}{2} + k_5 c_{51} c_{52} \\ s_{52} \\ -c_{52} s_{51} \\ c_{51} c_{52} \end{pmatrix}$$

Let $\bar{z} = \bar{f}_c(\zeta, \eta, C_1^0)$ where \bar{f}_c is the first 3 elements in the map f_c . Hence, substituting back into η -dynamics in (33) yields the normal form Σ_2^H

$$\Sigma_2^H : \begin{cases} \dot{\zeta}_1 = \zeta_2 \\ \dot{\zeta}_2 = v \\ \dot{\eta}_1 = \eta_2 \\ \dot{\eta}_2 = L_1 - M_{pp}^{-1} M_{bp}^T \zeta_2 + M_{pp}^{-1} D_3 \bar{f}_c \\ h_y = \zeta_1 \end{cases} \quad (35)$$

This proves Statement 1.

2) *Statement 2 Proof:* Σ_3 in the new coordinates after applying $H(\bar{x})$ (32) becomes this Σ_3^H

$$\Sigma_3^H : \dot{C}_1^0 = [\zeta_1] C_1^0 \quad (36)$$

Thus, Σ_2^H (35) interconnected with Σ_3^H (36) is equivalent to the system (1) with a linear relationship between virtual input v and output from the base spatial twist V_1^0 .

The zero dynamics of the network (Σ_2^H, Σ_3^H) are the internal dynamics when $h_y(t) \equiv 0 \forall t \geq 0$. This constraint is imposed for all times by setting the virtual input $v(t) = 0 \forall t \geq 0$ and the initial conditions of ζ -dynamics to be $(\zeta_1(0), \zeta_2(0)) = (0, 0)$. As a result, the linear differential equations of ζ admit the solution $(\zeta_1(t), \zeta_2(t)) = (0, 0) \forall t \geq 0$. This also leads to Σ_3^H (36) having a solution $C_1^0(t) = C_1^0(0) \forall t \geq 0$. Thus, the zero dynamics manifold \mathbb{Z} is then obtained as

$$\mathbb{Z} = \left\{ \eta(t) \in \mathbb{T}^6 \times \mathbb{R}^6, t \in \mathbb{R}_{\geq 0} \mid \dot{\eta}(t) = \begin{pmatrix} \eta_2(t) \\ F_\eta(\eta_1(t), \eta_2(t), 0, 0, C_1^0(0), \bar{f}_c(0, \eta(t), C_1^0(0))) \end{pmatrix} \right\} \quad (37)$$

Remark 2. In the original coordinates of system (Σ_2, Σ_3) , one can express the zero dynamics manifold (37) by transforming back the the initial conditions and the input constraint $v = 0$ from the normal form into the \bar{x} coordinates.

Hence, $\zeta_1(0) = V_1^0(0) = 0$ while the constraint $\zeta_2(0) = \dot{V}_1^0(0) = 0$ restricts the initial conditions of the dynamic extension states $z(0)^T$ and $q_a(0)$ to be a solution of (26) with $\dot{V}_1^0(0) = 0$. Let us call this solution f_{c_x} , then the zero dynamics manifold in the original coordinates \mathbb{Z}_x is defined by

$$\mathbb{Z}_x = \left\{ \bar{x}(t) \in \bar{\mathbb{X}}, t \in \mathbb{R}_{\geq 0} \mid \Sigma_2(\bar{x}; \bar{w}, C_1^0(0)), \bar{w} = -D_2^{-1} M_b E_2, \right. \\ \left. C_1^0(0) \in SE(3), V_1^0(0) = 0, (z(0), q_a(0))^T = f_{c_x} \right\} \quad (38)$$

What is remaining to complete the proof is to study the stability of the zero dynamics. When we restrict $\eta \in \mathbb{Z}$ we get,

$$\dot{\eta}_1 = \eta_2$$

$$\dot{\eta}_2 = \tilde{M}_{pp}^{-1} (-D_f \eta_1 - \text{col}(\tilde{S}_j^T (\tilde{M}_{B_j}^0 \dot{S}_j + \dot{M}_{B_j}^0 \tilde{S}_j) \eta_{2j}) \\ + \tilde{S}_p^T \text{col}(\tilde{M}_{B_j} G^0) + D_3 \tilde{z}) \\ = \tilde{M}_{pp}(\eta_1)^{-1} (-D_f \eta_2 - \tilde{C}(\eta_1, \eta_2) \eta_2 - \tilde{g}_p(\eta_1) + D_3(\eta_1) \tilde{z}) \quad (39)$$

The superscript (\cdot) donates the value of the corresponding variable evaluated at $(C_1^0(t), \zeta_1(t), \zeta_2(t)) = (C_1^0(0), 0, 0)$. \tilde{C} is the Coriolis matrix which is linear in passive joint velocities η_2 and given by

$$\tilde{C} = \text{blkdiag}(\tilde{C}_2(\eta_{12}, \eta_{22}), \tilde{C}_3(\eta_{13}, \eta_{23}), \tilde{C}_4(\eta_{14}, \eta_{24}))$$

$$\tilde{C}_j = \begin{pmatrix} S_{j1}^T M_{B_j}^0 \dot{S}_{j1} - S_{j1}^T \text{ad}_{S_{j2}}^T M_{B_j}^0 S_{j1} \eta_{2j2} & S_{j1}^T M_{B_j}^0 \dot{S}_{j2} - S_{j1}^T \text{ad}_{S_{j2}}^T M_{B_j}^0 S_{j2} \eta_{2j2} \\ S_{j2}^T M_{B_j}^0 \dot{S}_{j1} - S_{j2}^T \text{ad}_{S_{j1}}^T M_{B_j}^0 S_{j1} \eta_{2j1} & S_{j2}^T M_{B_j}^0 \dot{S}_{j2} - S_{j2}^T \text{ad}_{S_{j1}}^T M_{B_j}^0 S_{j2} \eta_{2j1} \end{pmatrix} \quad (40)$$

where $j = 2, 3, 4$.

A suitable choice of positive definite smooth Lyapunov candidate is the total energy of the rigid bodies connected by the passive joints comprising the internal dynamics $U_\eta(\eta) : \mathbb{Z} \rightarrow \mathbb{R}_{>0} \forall \eta \neq \eta_e, U_\eta(\eta_e) = 0 \forall \eta_e \in \mathbb{D}_{x_e}^{[i]}$

$$U_\eta = \frac{1}{2} \eta_2^T \tilde{M}_{pp} (\eta_1 - \eta_{1e}) \eta_2 + \tilde{U}(\eta_1 - \eta_{1e})$$

where $\tilde{U}(\eta_1 - \eta_{1e})$ is the potential energy of the passive dynamics in the manifold $\eta \in \mathbb{Z}$ whose time derivative is

$$\dot{\tilde{U}} = \eta_2^T \frac{\partial \tilde{U}}{\partial (\eta_1 - \eta_{1e})} \\ = -\eta_2^T \tilde{S}_p^T (\eta_1 - \eta_{1e}) \text{col}(\tilde{M}_{B_j} (\eta_1 - \eta_{1e}) G^0) = \eta_2^T \tilde{g}_p$$

where $G^0 = \text{col}(0_5, -9.81 \text{ m/s}^2)$. Taking the time derivatives of U_η yields

$$\dot{U}_\eta = \eta_2^T \tilde{M}_{pp} \dot{\eta}_2 + \frac{1}{2} \eta_2^T \dot{\tilde{M}}_{pp} \eta_2 + \dot{\tilde{U}} \\ = \eta_2^T \left(\frac{1}{2} \dot{\tilde{M}}_{pp} - \tilde{C} \right) \eta_2 \\ - \eta_2^T D_f \eta_2 - \eta_2^T \tilde{g}_p + \eta_2^T D_3 \tilde{z} + \eta_2^T \tilde{g}_p$$

Since $\frac{1}{2} \dot{\tilde{M}}_{pp} - \tilde{C}$, with $\dot{\tilde{M}}_{pp}$ and \tilde{C} respectively given in Sec. A and (40), is skew-symmetric, \dot{U}_η reduces to

$$\dot{U}_\eta = -\eta_2^T D_f \eta_2 + \eta_2^T D_3 \tilde{z}$$

Thus for asymptotic stability of η_e , \tilde{z} must satisfy

$$\eta_2^T D_3 \tilde{z} < \eta_2^T D_f \eta_2$$

Since the quadratic form $\eta_2^T D_f \eta_2$ can be bounded by

$$\lambda_{\min}(D_f) \|\eta_2\|^2 \leq \eta_2^T D_f \eta_2 \leq \lambda_{\max}(D_f) \|\eta_2\|^2$$

Applying Cauchy–Schwarz inequality to bound $|\eta_2^T D_3 \tilde{z}| \leq \|\eta_2\| \|D_3 \tilde{z}\|$ yields the bounds on $\tilde{z} \forall \eta \in \mathbb{Z} - \{\eta_e\}$ to be (8) in original coordinates, where also this norm property $\|D_3 \tilde{z}\| \leq \|D_3\| \|\tilde{z}\|$ is used. The proof is concluded.

F. Proof of Proposition 2

We construct the state feedback for the virtual input v which locally asymptotically stabilizes $\Sigma_\zeta : \dot{\zeta}_1 = \zeta_2, \dot{\zeta}_2 = v$ composed with Σ_3^H at $(\zeta_{1e}, \zeta_{2e}, C_{1e}^0)$. Thus, from Theorem 10.3.1 in [23], the cascaded interconnection of the autonomous system Σ_ζ composed with Σ_3^H , and the internal dynamics Σ_η is guaranteed to be LAS in $\mathbb{U}_{\bar{x}_e} \times SE(3)$, given the result on the stability of the zero dynamics stated in Theorem 1.

Consider the system Σ_3^H (36). The goal is to find a feedback law for the input ζ_1 to stabilize the equilibrium C_{1e}^0 . To this end, we choose the positive definite smooth Lyapunov candidate $U_b(C_1^0) : SE(3) \rightarrow \mathbb{R}_{>0} \forall C_1^0 \neq C_{1e}^0, U_b(C_{1e}^0) = 0$ to be

$$\begin{aligned} U_b(C_1^0(t)) &= \frac{1}{2} \|C_0^{1e} C_1^0(t) - I\|_F^2 \\ &= \frac{1}{2} \text{tr} \left((C_0^{1e} C_1^0(t) - I)^T (C_0^{1e} C_1^0(t) - I) \right) \end{aligned}$$

where $\|\cdot\|_F$ is the Frobenius norm and $\text{tr}(\cdot)$ denotes the trace. The term $C_0^{1e} C_1^0(t)$ is the left-trivialized error on $SE(3)$. Define the variable E_c as

$$E_c = C_0^{1e} C_1^0(t) - I \quad (41)$$

Taking the time derivatives of the $U_b(C_1^0)$ along the trajectories of C_1^0 while simplifying using properties of the trace yields

$$\begin{aligned} \dot{U}_b(C_1^0(t)) &= \frac{1}{2} \frac{d}{dt} \text{tr} (E_c^T E_c) = \frac{1}{2} \text{tr} \left(\frac{d}{dt} E_c^T E_c + E_c^T \frac{d}{dt} E_c \right) \\ &= \frac{1}{2} \text{tr} \left(\frac{d}{dt} E_c^T E_c \right) + \frac{1}{2} \text{tr} \left(E_c^T \frac{d}{dt} E_c \right) \\ &= \frac{1}{2} \text{tr} \left(E_c^T \frac{d}{dt} E_c \right)^T + \frac{1}{2} \text{tr} \left(E_c^T \frac{d}{dt} E_c \right) \\ &= \text{tr} \left(E_c^T \frac{d}{dt} E_c \right) \end{aligned}$$

Since $\frac{d}{dt} E_c$ is given by

$$\dot{E}_c = C_0^{1e} \frac{d}{dt} C_1^0(t) = C_0^{1e} [\zeta_1] C_1^0(t) \quad (42)$$

Hence

$$\begin{aligned} \dot{U}_b(C_1^0(t)) &= \text{tr} \left(E_c^T C_0^{1e} [\zeta_1] C_1^0(t) \right) = \text{tr} \left(C_1^0(t) E_c^T C_0^{1e} [\zeta_1] \right) \\ &= \text{tr} \left((C_0^{1e})^T E_c (C_1^0)^T [\zeta_1] \right) \end{aligned}$$

By using the fact that if $[b] \in se(3)$, $A \in \mathbb{R}^{4 \times 4}$ then this trace property holds $\text{tr} (A^T [b]) = \text{tr} (P_{se(3)}^T(A) [b])$ where $P_{se(3)}(A)$ projects the matrix A on $se(3)$ as follows

$$P_{se(3)}(A) = \begin{pmatrix} \frac{1}{2}(A_{[1:3,1:3]} - A_{[1:3,1:3]}^T) & A_{[1:3,4]} \\ 0_{1 \times 3} & 0 \end{pmatrix}$$

where $A_{[a:b,c:d]}$ constructs a new matrix by extracting from matrix A the rows number a to b and columns number c to d , \dot{U}_b hence becomes

$$\begin{aligned} \dot{U}_b(C_1^0(t)) &= \text{tr} \left(P_{se(3)}^T \left((C_0^{1e})^T E_c (C_1^0)^T \right) [\zeta_1] \right) \\ &= \hat{P}_{se(3)}^T \left((C_0^{1e})^T E_c (C_1^0)^T \right) L \zeta_1 \end{aligned}$$

where $L = \text{diag}(2, 2, 2, 1, 1, 1)$. Now let the input ζ_1 be

$$\zeta_1 = -K_p \hat{P}_{se(3)} \left((C_0^{1e})^T E_c (C_1^0)^T \right) =: \zeta_{1e} \quad (43)$$

where the diagonal gain matrix $K_p > 0 \in \mathbb{R}^{6 \times 6}$ and $\hat{\cdot} : se(3) \rightarrow \mathbb{R}^6$ denotes the inverse of the isomorphism $[\cdot]$. Substituting (43) makes \dot{U}_b take this quadratic form

$$\begin{aligned} \dot{U}_b(C_1^0(t)) &= -\hat{P}_{se(3)}^T \left((C_0^{1e})^T E_c (C_1^0)^T \right) L K_p \hat{P}_{se(3)} \left((C_0^{1e})^T E_c (C_1^0)^T \right) \\ &= -\| [K_p^{\frac{1}{2}} \hat{P}_{se(3)} \left((C_0^{1e})^T E_c (C_1^0)^T \right)] \|_F^2 < 0 \quad \forall E_c \neq 0 \end{aligned}$$

Now, we follow a backstepping strategy to stabilize the ζ_1 -dynamics at the equilibrium ζ_{1e} (43) using the input ζ_2 . Consider the positive definite smooth Lyapunov candidate $U_{\zeta_1}(C_1^0, \zeta_1) : SE(3) \times \mathbb{R}^6 \rightarrow \mathbb{R}_{>0}, \forall C_1^0 \neq C_{1e}^0$ and $\forall \zeta_1 \neq \zeta_{1e}$, with $U_{\zeta_1}(C_{1e}^0, \zeta_{1e}) = 0$

$$U_{\zeta_1}(C_1^0, \zeta_1) = U_b + \frac{1}{2} \|\zeta_1 - \zeta_{1e}\|^2$$

Taking the time derivatives of U_{ζ_1} gives

$$\dot{U}_{\zeta_1}(C_1^0, \zeta_1) = \dot{V}_1 + (\dot{\zeta}_1 - \dot{\zeta}_{1e})^T (\zeta_1 - \zeta_{1e})$$

hence by substituting the dynamics of ζ_1 (35), i.e., $\dot{\zeta}_1 = \zeta_2$

$$\dot{U}_{\zeta_1}(C_1^0, \zeta_1) = \dot{V}_1 + (\zeta_2 - \dot{\zeta}_{1e})^T (\zeta_1 - \zeta_{1e})$$

and selecting the input ζ_2 as

$$\zeta_2 = \dot{\zeta}_{1e} + \bar{\zeta}_2$$

thus the derivatives of U_{ζ_1} reads as

$$\dot{U}_{\zeta_1}(C_1^0, \zeta_1) = \dot{V}_1 + \bar{\zeta}_2^T (\zeta_1 - \zeta_{1e})$$

Setting $\bar{\zeta}_2$ to be $\bar{\zeta}_2 = -K_d (\zeta_1 - \zeta_{1e})$, where the diagonal gain matrix $K_d > 0 \in \mathbb{R}^{6 \times 6}$, renders \dot{U}_{ζ_1} negative definite $\forall (C_1^0, \zeta_1) \neq (C_{1e}^0, \zeta_{1e})$

$$\dot{U}_{\zeta_1}(C_1^0, \zeta_1) = \dot{V}_1 - (\zeta_1 - \zeta_{1e})^T K_d (\zeta_1 - \zeta_{1e}) < 0$$

The total control law for ζ_2 is

$$\zeta_2 = \dot{\zeta}_{1e} - K_d (\zeta_1 - \zeta_{1e}) =: \zeta_{2e} \quad (44)$$

This step is repeated once again to design a controller v that stabilizes the ζ_2 -dynamics (35) at the equilibrium ζ_{2e} with the Lyapunov candidate $U_{\zeta_2}(C_1^0, \zeta_1, \zeta_2)$ given by

$$U_{\zeta_2}(C_1^0, \zeta_1, \zeta_2) = U_b(C_1^0) + U_{\zeta_1}(C_1^0, \zeta_1) + \frac{1}{2} \|\zeta_2 - \zeta_{2e}\|^2$$

The equation for the virtual input v is thus obtained as

$$v = \dot{\zeta}_{2e} - K_a(\zeta_2 - \zeta_{2e}) \quad (45)$$

where K_a is a diagonal gain matrix $K_a > 0 \in \mathbb{R}^{6 \times 6}$.

The time derivatives of ζ_{1e} are functions of the first time derivative of the error E_c (41), i.e. \dot{E}_c (42), and

$$\ddot{E}_c = C_0^{1e} \left([\dot{\zeta}_2] + [\dot{\zeta}_1]^2 \right) C_1^0$$

Hence

$$\begin{aligned} \dot{\zeta}_{1e} &= -K_p \hat{P}_{se(3)} \left((C_0^{1e})^T \left(\dot{E}_c (C_1^0)^T + E_c (C_1^0)^T [\zeta_1]^T \right) \right) \\ \ddot{\zeta}_{1e} &= -K_p \hat{P}_{se(3)} \left((C_0^{1e})^T \left(\ddot{E}_c (C_1^0)^T + 2\dot{E}_c (C_1^0)^T [\zeta_1]^T + E_c (C_1^0)^T \left(([\zeta_1]^T)^2 + [\zeta_2]^T \right) \right) \right) \end{aligned} \quad (46)$$

After some algebraic manipulations of (44) and (45), the virtual control v can be rewritten as

$$v = \ddot{\zeta}_{1e} + \bar{K}_d(\dot{\zeta}_{1e} - \dot{\zeta}_2) + \bar{K}_a(\zeta_{1e} - \zeta_1)$$

where $\bar{K}_a > 0 \in \mathbb{R}^{6 \times 6}$, $\bar{K}_d > 0 \in \mathbb{R}^{6 \times 6}$ are diagonal gain matrices. They are related to K_a and K_d by

$$\bar{K}_a = K_d K_a, \quad \bar{K}_d = K_d + K_a$$

If the error states are defined as

$$e_{s1}(t) := \zeta_{1e} - \zeta_1, \quad e_{s2}(t) := \dot{\zeta}_{1e} - \dot{\zeta}_2$$

then a linear error system with a state $e_s = (e_{s1} \ e_{s2})^T$ and a pair (A, B) given in Proposition 2 results. The gain matrices \bar{K}_d and \bar{K}_a can thus be tuned to exponentially stabilize its origin by rendering $(A - BK)$ Hurwitz.

Remark 3. *Observe that to eliminate the steady-state error in the convergence of $e_s(t)$ to zero, which may be present due to parametric uncertainty, an integral term can be added to v as*

$$v = \ddot{\zeta}_{1e} + \bar{K}_d(\dot{\zeta}_{1e} - \dot{\zeta}_2) + \bar{K}_a(\zeta_{1e} - \zeta_1) + K_I \int (\zeta_{1e} - \zeta_1) dt$$

where $K_I = K_I^T > 0 \in \mathbb{R}^{6 \times 6}$ is the integral gain matrix.

This concludes the proof.